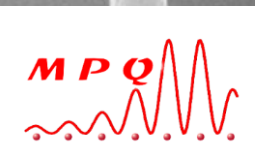


Metamaterials for THz detection

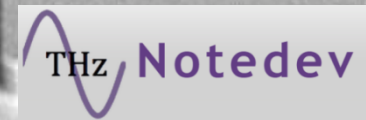
Carlo Sirtori

Y. Todorov, D. Palaferri, C. Belacel, A. Vasanelli, S. Barbieri, D. Gacemi, I. Favero
*Laboratoire Matériaux et Phénomènes Quantiques, Université Paris Diderot –
CNRS UMR 7162, 75205 Paris Cedex 13, France*

New Frontiers in 2D materials: Approaches & Applications
15-20 January 2017, Villard-de-Lans, FRANCE



ADEQUATE



Collaborators

Epitaxial Growth



UNIVERSITY OF LEEDS

L. H. Li, A. G. Davies,
E. H. Linfield (THz and Mid-IR QWIPs)

*School of Electronic and Electrical Engineering, University of Leeds,
Leeds LS2 9JT, United Kingdom*



G. Biasiol (Mid-IR QWIPs)

*IOM CNR, Laboratorio TASC, Area Science Park,
I-34149 Trieste, Italy*

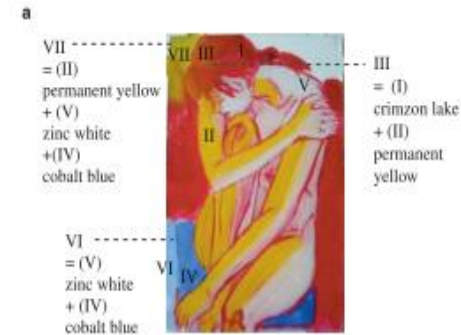
THz applications

- **Terahertz : 1 – 5 THz 300 – 30 μ m**

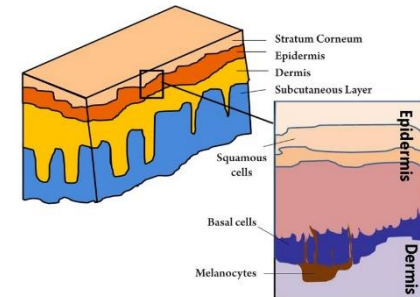
Imaging (cw sources, incoherent detection)

focal planar arrays in conjunction with cw sources

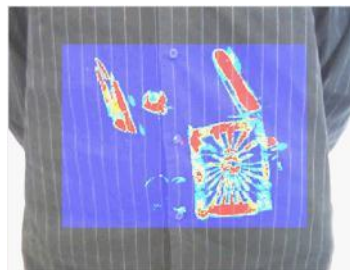
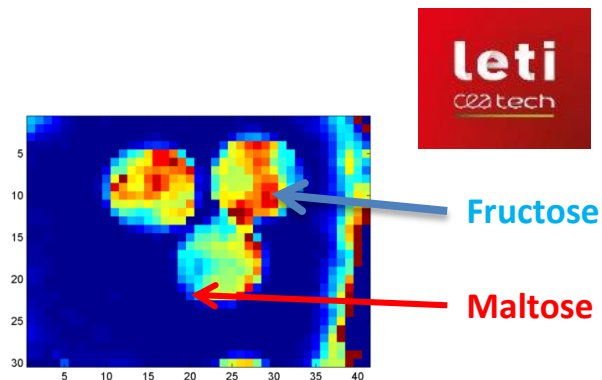
- *Material inspection*
- *Security*
- *Analytical imaging (Food)*
- *Microscopy*
- *Medical (tumor detection)*



*K. Fukunaga et. al.
IEICE Electronics Express, 4, 8, p. 258 (2007)*



*Calvin Yu, et al,
Quant Imaging Med Surg. 2012 Mar; 2(1): 33–45.*



Photonic detectors in the THz/MiR

- Photonic (energy) detectors have high dark current
→ cryogenic operation

$\lambda=10\mu\text{m}$, $T \sim 80\text{K}$



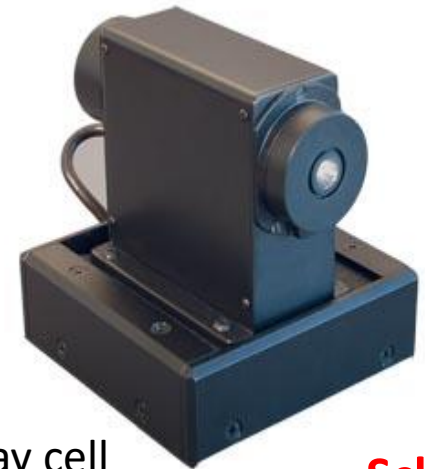
Image: Judson website

THz: $\lambda=100\mu\text{m}$, $T \sim 4\text{K}$



QMC Bolometer

Room temperature



Golay cell

- Schotky

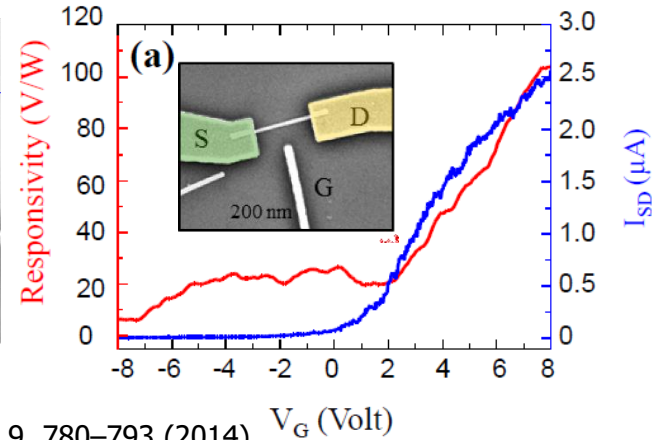
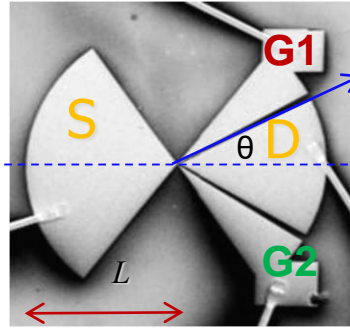
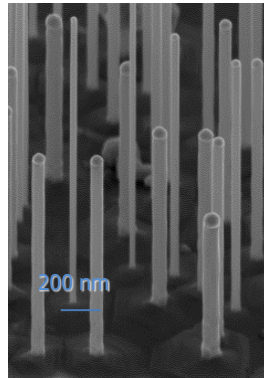
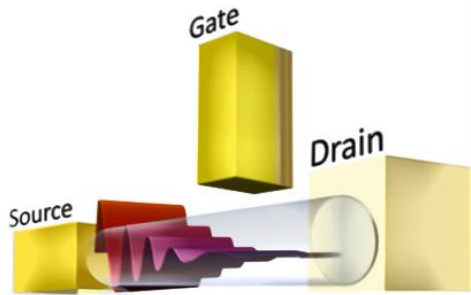
Same detectors for the past 30-40 years

- Good detectors !
- In continuous evolution

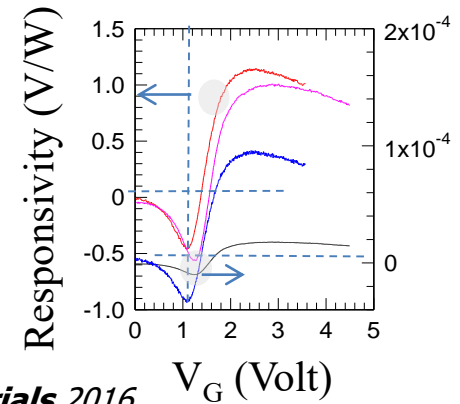
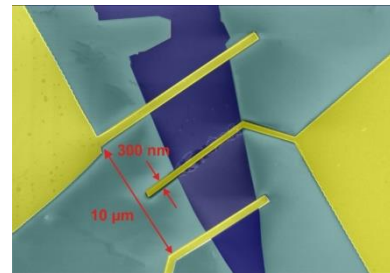
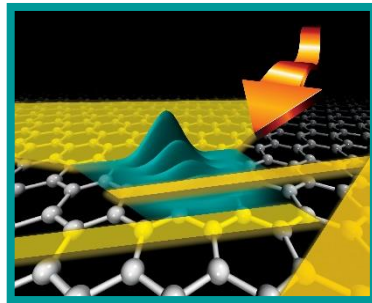
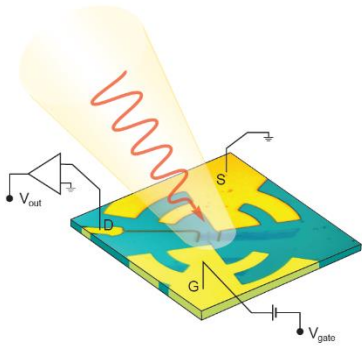
Room Temperature Terahertz Nanodetectors: Nanowires, Graphene, Black Phosphorus

M.S. Vitiello et al. Nano Letters 2012; APL Materials 2015;

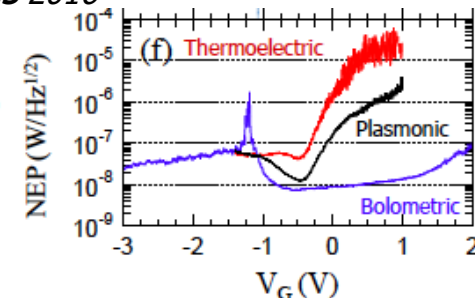
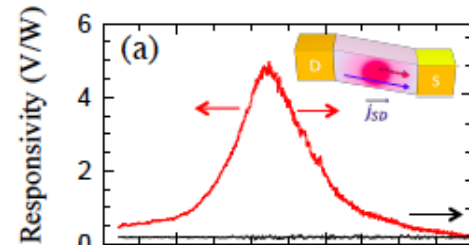
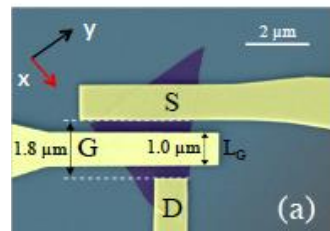
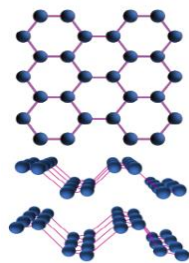
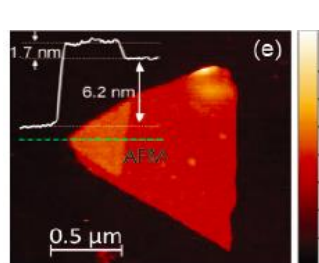
M. Eisele et al. Nature Photonics 2014



Koppens, Mueller, Avouris, A. C. Ferrari, M. S. Vitiello & M. Polini, Nature Nanotechnology 9, 780–793 (2014)

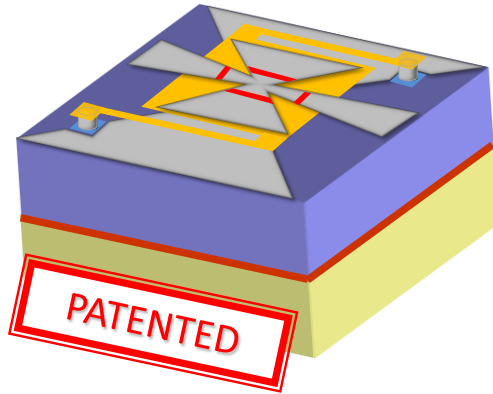


L. Viti et al. Advanced Materials 2015; Viti et al. Scientific Reports 2016; Advanced Materials 2016

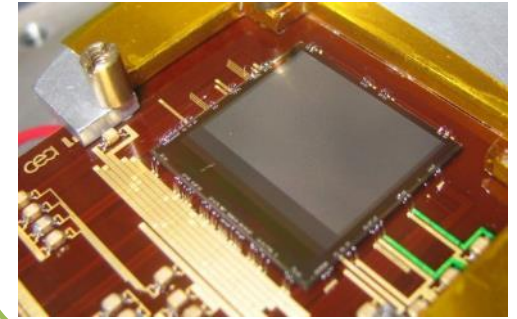


- **LETI THZ BOLOMETER ARRAY FABRICATION**

- **FABRICATED ANTENNA-COUPLED M-BOLOMETER FPAs**

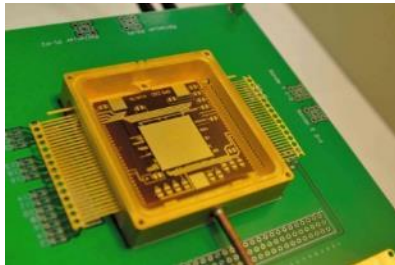


■ 320x240 pixel FPA

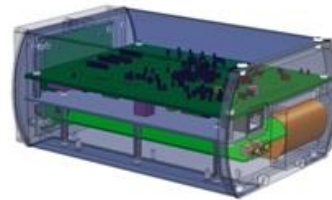


- FPA integrated in Ethernet video output cameras

Specific vacuum packaging



FPGA front-end electronics



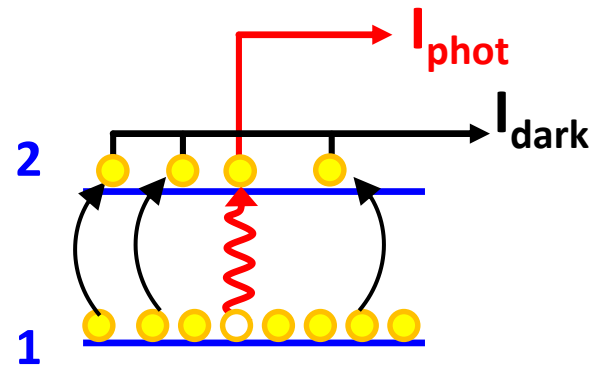
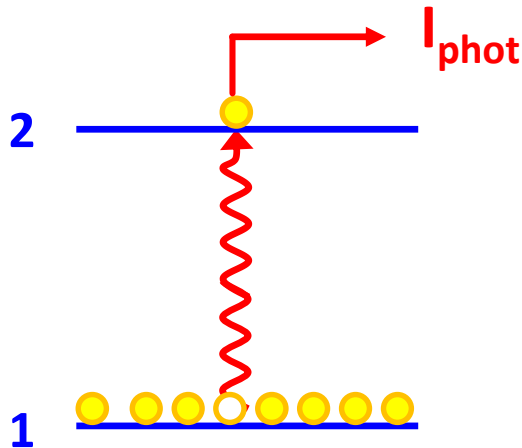
Camera housing



Photonic detection in the THz \rightarrow Dark current

The dark current is an activated process:

$$I_{dark} \propto \exp(-E_{act}/kT) \quad \text{where} \quad E_{act} \sim E_{12}$$

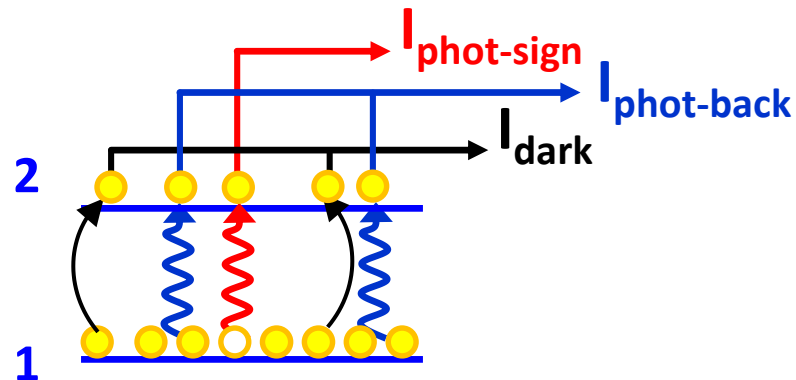


The signal is washed out by the dark current noise \rightarrow Detector must be cooled!

Background photocurrent

In the far infrared photons are at the equilibrium with the earth temperature
300K Black-Body $\sim 300 \text{ Wm}^{-2}$

For cold detectors there is a net flux of photon coming from the background



The total current in the detector is $I_{\text{tot}} = I_{\text{phot}} + I_{\text{phot-back}} + I_{\text{dark}}$

$I_{\text{phot-back}}$ contributes to the noise!

Current noise $\bar{I}_v = \sqrt{2eg I_{\text{tot}} \Delta\nu}$

Background limited detectivity

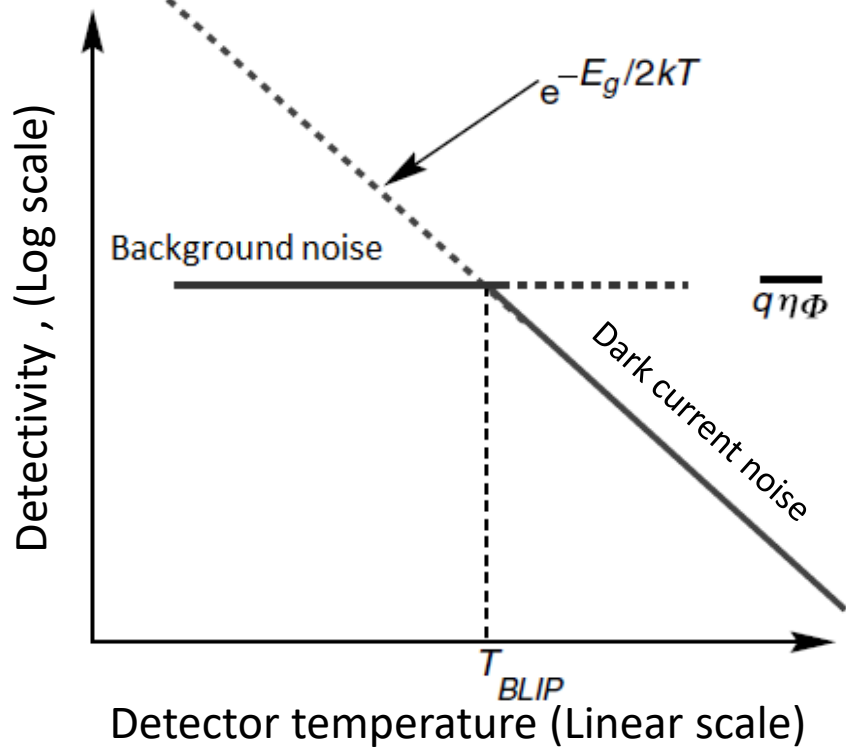
$$I_{tot} = \underbrace{I_{\cancel{\text{phot-sign}}} + I_{\text{phot-back}}}_{I_{\text{phot}}} + I_{\text{dark}}$$

Background limited Temperature:

$$I_{\text{dark}}(T_{BLIP}) = I_{\text{phot}} = I_{\text{tot}} - I_{\text{dark}}$$

$$I_{\text{tot}} = 2I_{\text{dark}}(T_{BLIP})$$

T_{BLIP} is the operating temperature!



$$I_{\text{phot-back}} \sim A_{\text{device}} \times \text{photon flux}$$

$$I_{\text{dark}} \sim A_{\text{device}} \times \exp(-E_{12}/k_B T)$$

Figure of merits for detectors

Photoconductor detectors

$$\bar{I}_v = \sqrt{2eg I_{tot} \Delta\nu}$$

Responsivity

$$R = \frac{I_{phot}}{P_{in}} \quad [\text{A/W}]$$

Noise Equivalent Power

$$NEP = \frac{\text{Current noise}}{\text{Responsivity}} = \frac{\bar{I}_v}{R} \quad [\text{W}/(\text{Hz}^{1/2})]$$



Detectivity

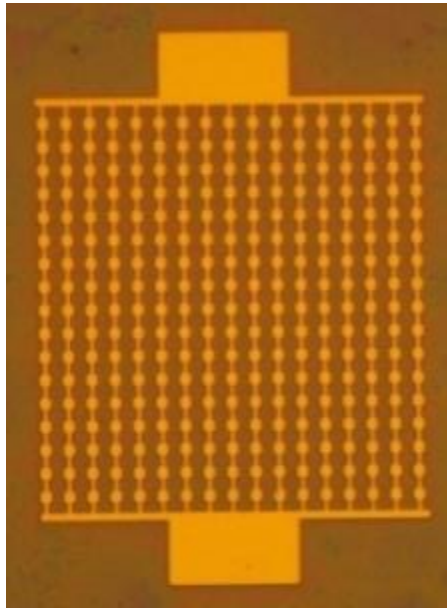
$$D^* = \frac{\sqrt{A f}}{NEP} \quad [\text{cm Hz}^{1/2}/\text{W}]$$



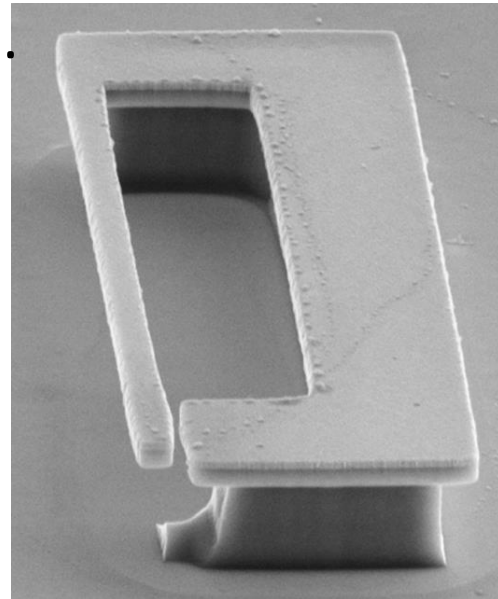
Outline

1. Antenna and circuit concepts for Quantum THz detectors
2. Optomechanical THz detection using metamaterials

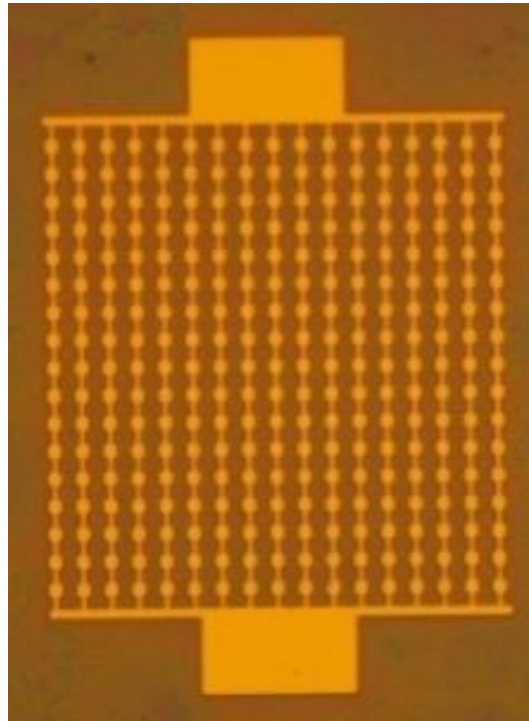
1.



2.



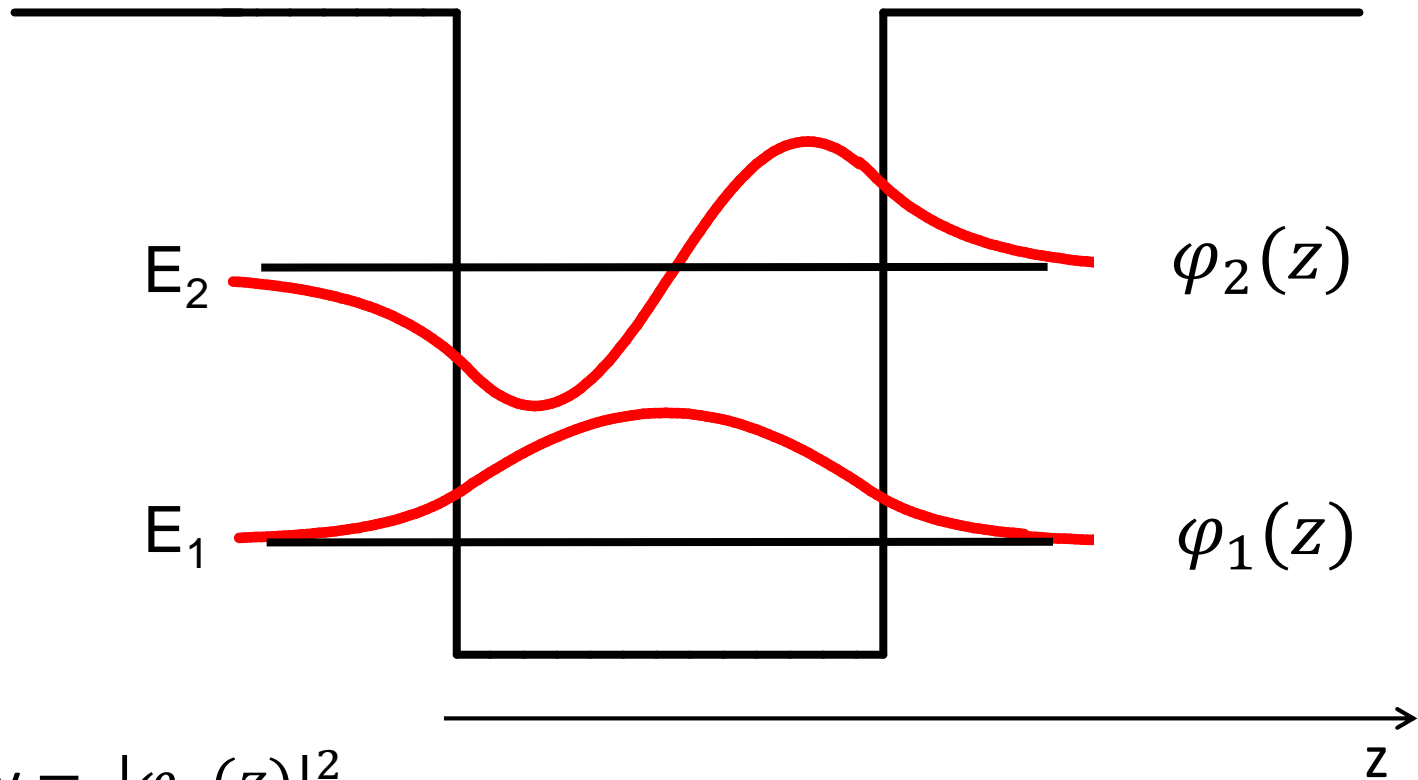
Antenna coupled microcavities for Quantum THz detectors



Quantum well potential

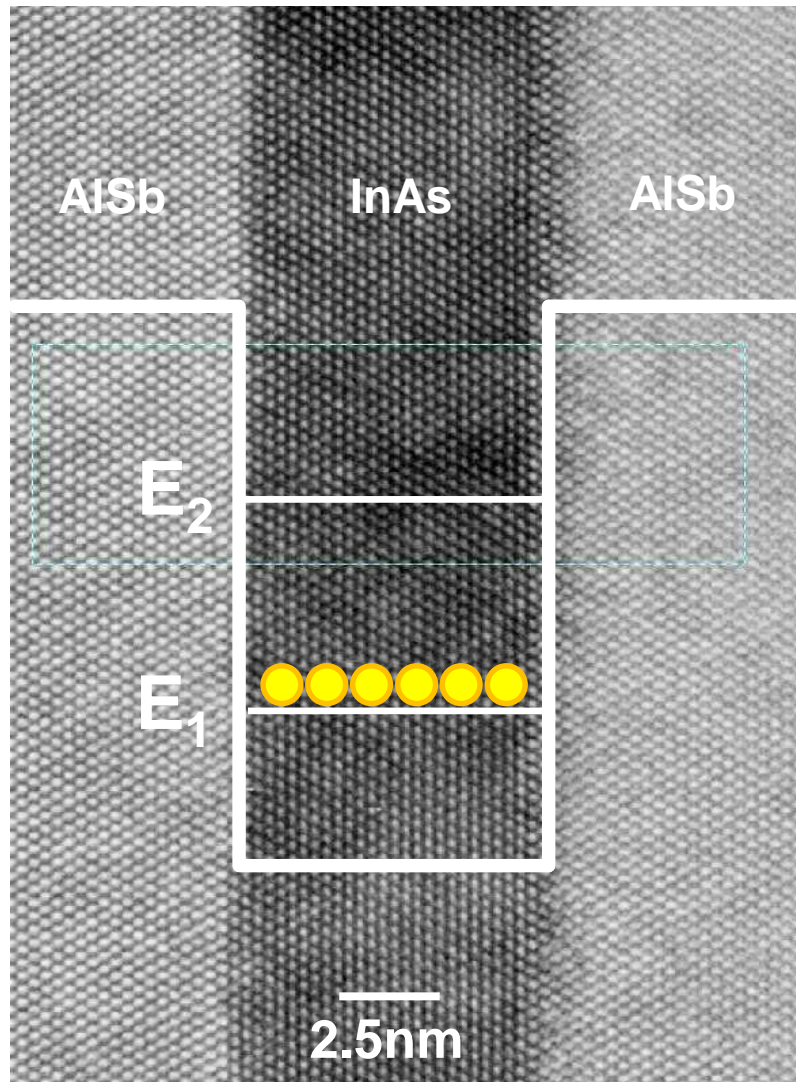
The Schrodinger equation

$$H \psi = E \psi \quad \text{with} \quad H = \frac{p^2}{2m^*} + V(z)$$



Probability = $|\varphi_n(z)|^2$

Quantum potential in semiconductors

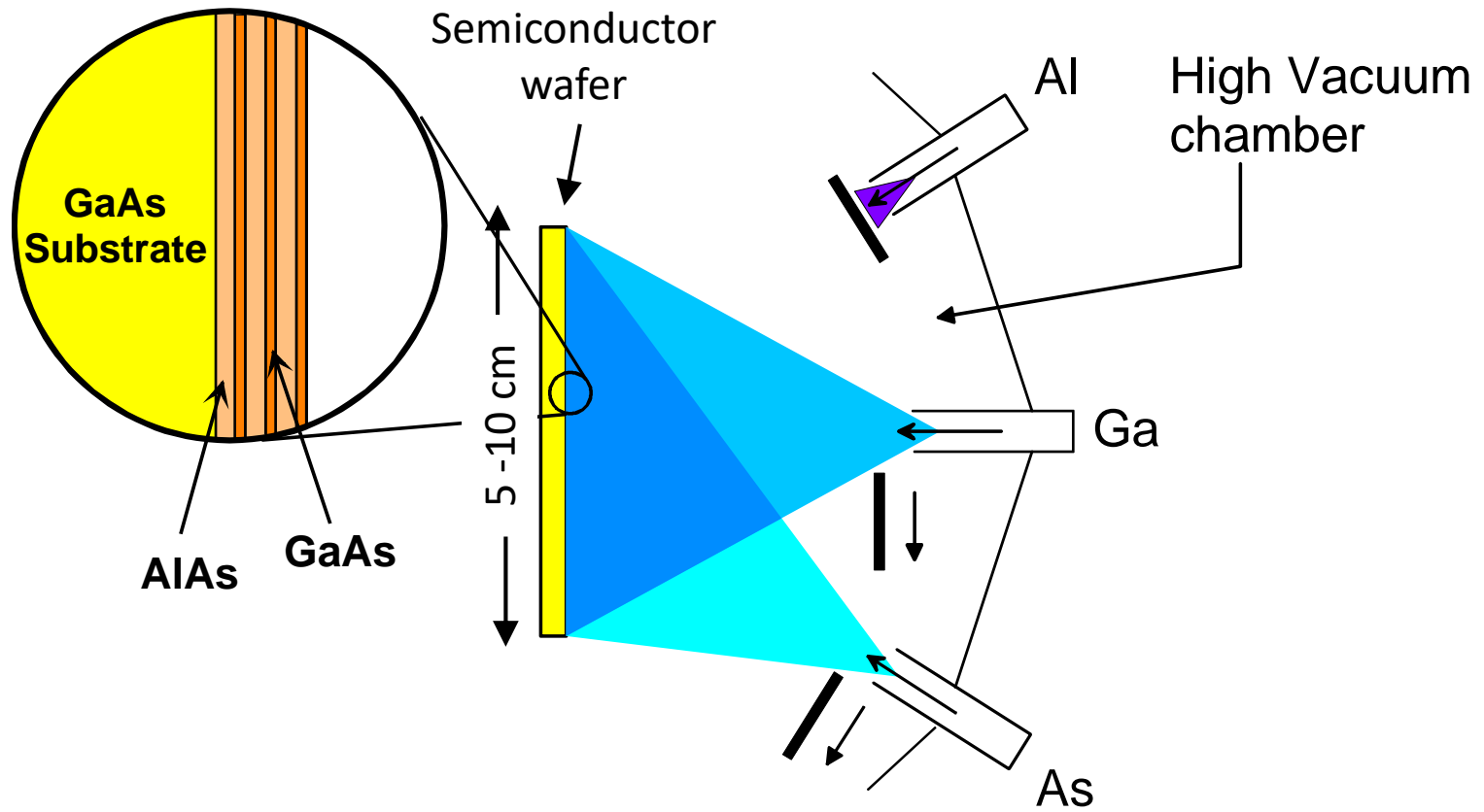


**Epitaxially grown material
with very abrupt interfaces**

**The quantum well is the
elementary constituent of
more complex potentials**

Molecular beam epitaxy

Different semiconductors may have the same lattice constant and can be grown into a single crystal structure

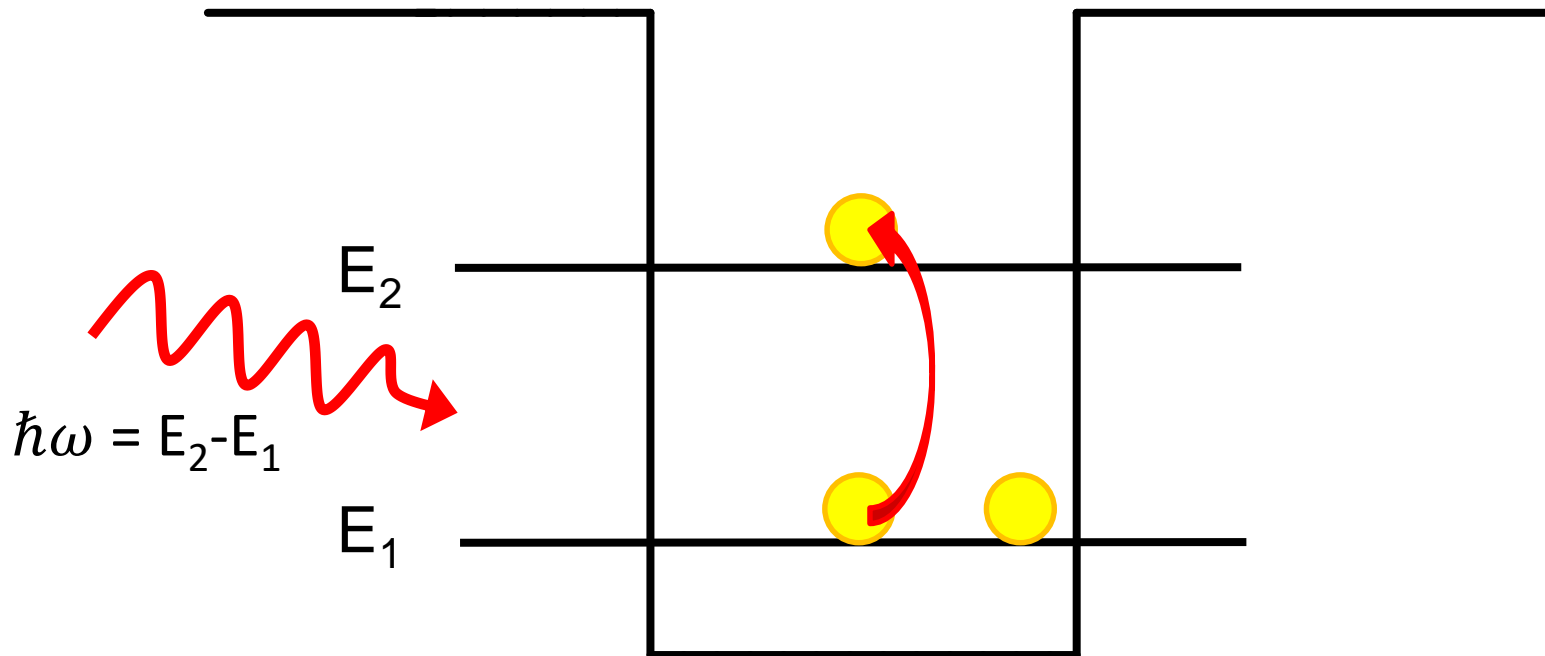


Deposition of atomic layer after atomic layer

Light-matter interaction in quantum quantum wells

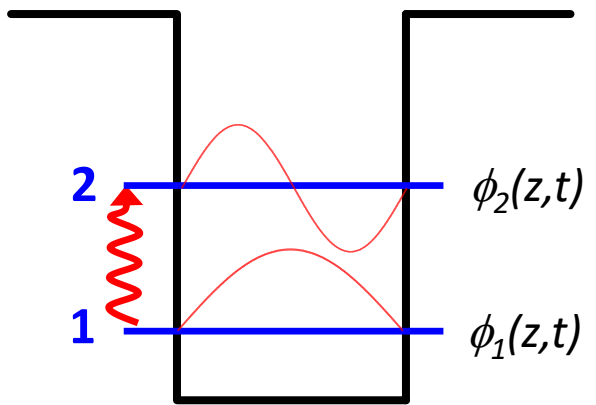
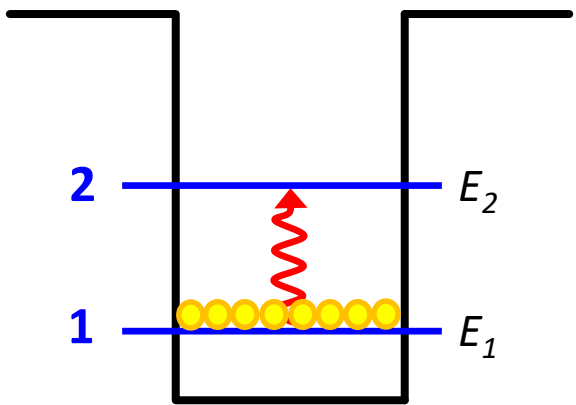
Light-matter interaction

Energy exchange between a photon and the quantum structure



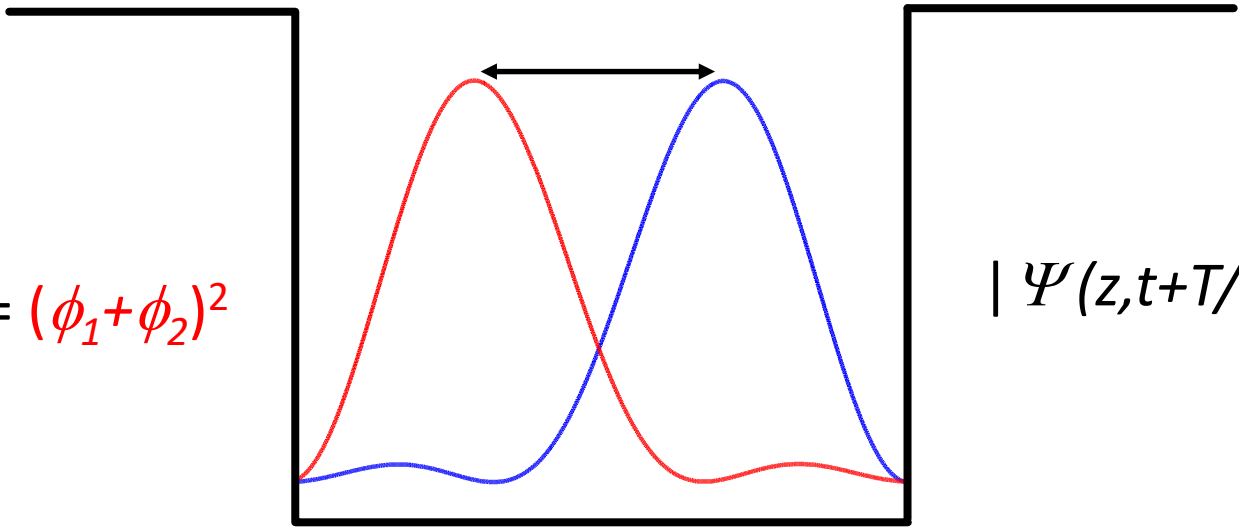
$E_2 - E_1 < 1\text{eV} \rightarrow$ The transitions are typically in the infrared

Intersubband transitions



$$|\Psi(z,t)|^2 = |\phi_1(z,t) + \phi_2(z,t)|^2$$

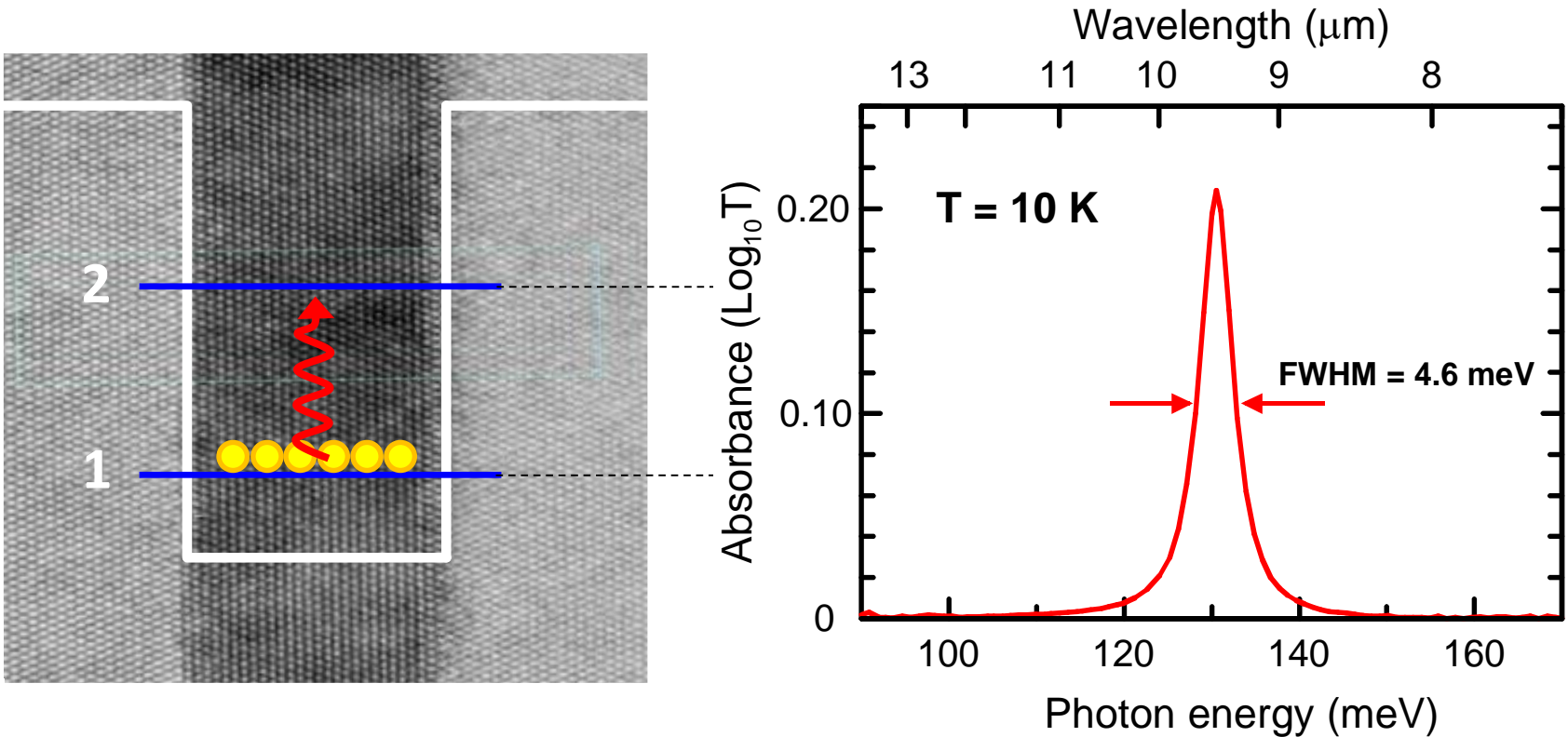
$$|\Psi(z,t)|^2 = (\phi_1 + \phi_2)^2$$



$$|\Psi(z,t+T/2)|^2 = (\phi_1 - \phi_2)^2$$

Intersubband transitions (absorption)

The absorption of a photon is related only to the energy difference between the subbands and does not depend on $k_{//}$



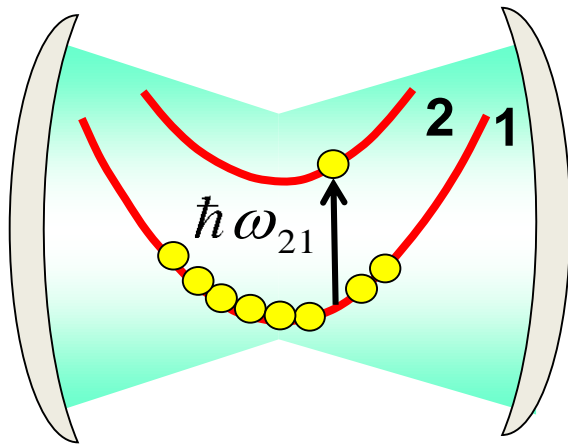
$$E_{n,k} - E_{m,k} = \Delta E_{nm} \quad \forall k$$

Absorption peaks like in 3D confined potentials: atoms

Many-body quantum optics

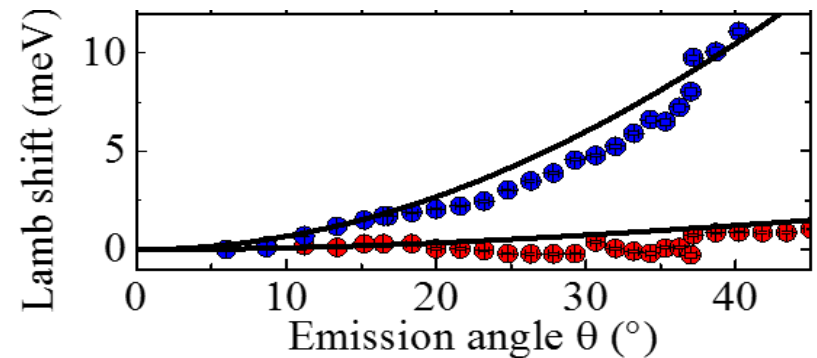
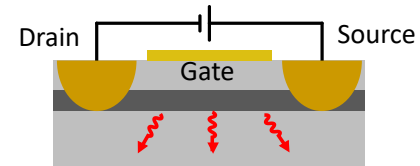
Fundamental investigations

Ultra strong coupling



Cooperative Lamb Shift

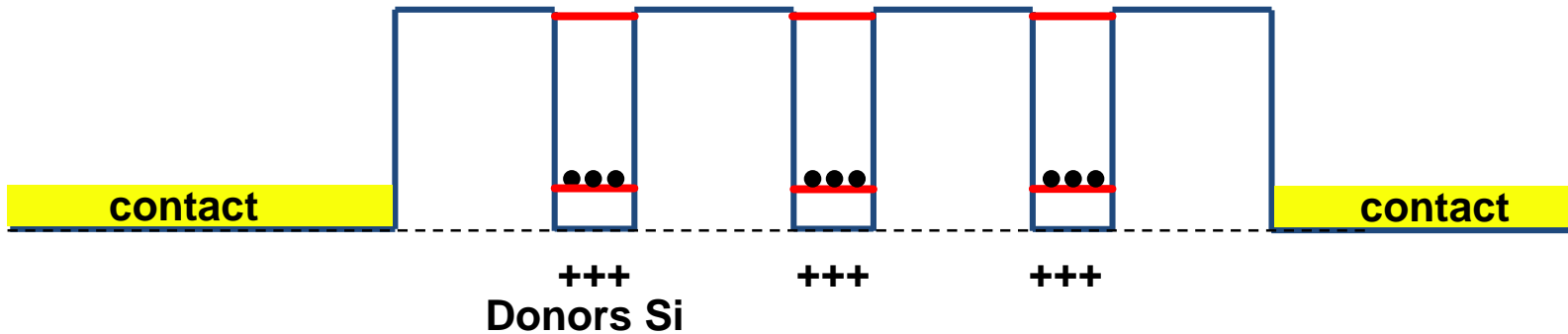
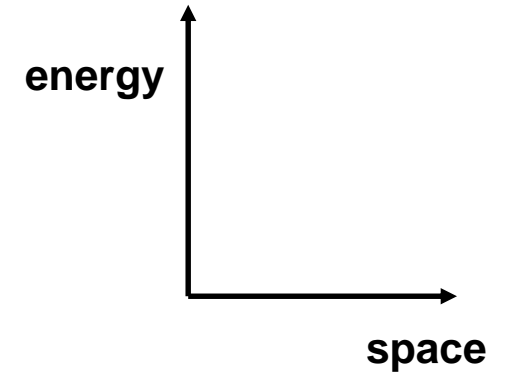
Superradiance



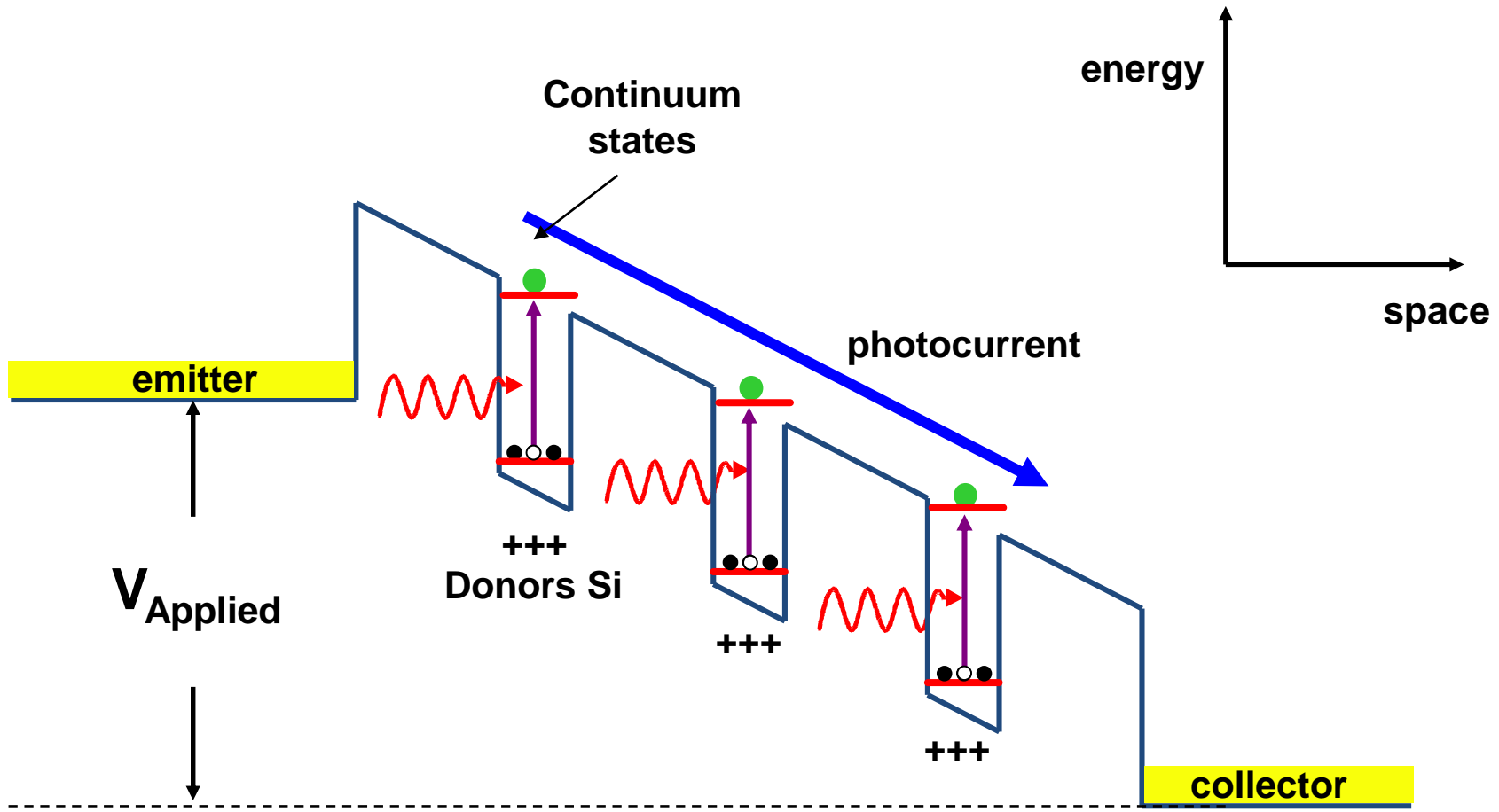
Quantum well infrared photodetector

Quantum Well Infrared Photo-detector (QWIP)

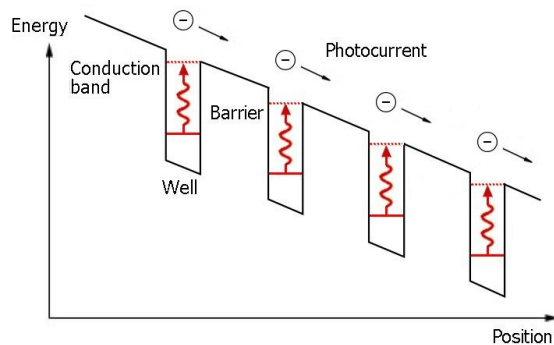
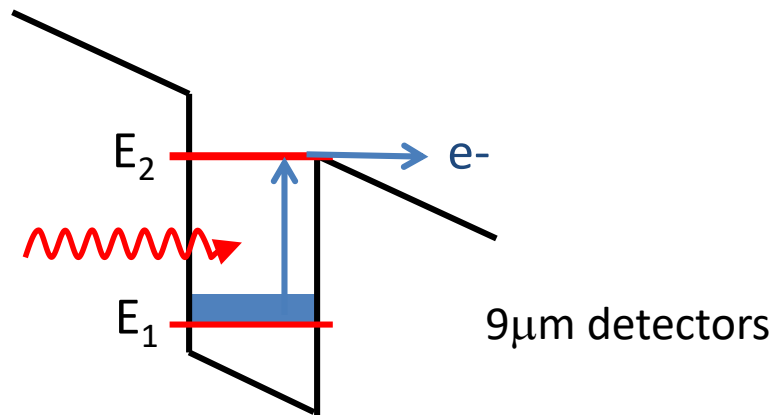
Set of uncoupled quantum well with the excited states very close to the barrier top



Quantum Well Infrared Photo-detector (QWIP)



Quantum well infrared photodetector (QWIP)



THz ($\lambda=100\mu\text{m}$) ?

B. F. Levine (Bell Labs, 1987)

H. Schneider, H. C. Liu,
Quantum well infrared photodetectors: Physics and applications (Springer, Berlin, 2007).

TeraHertz QWIP

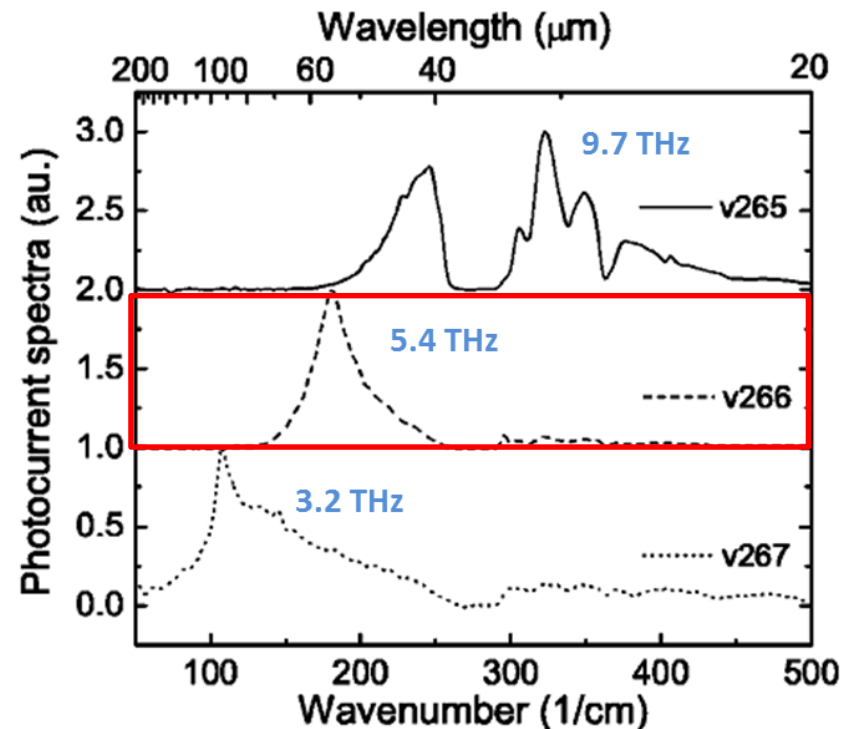
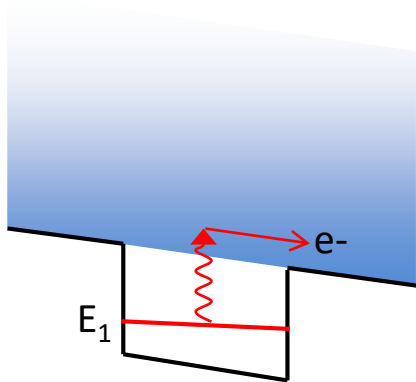
APPLIED PHYSICS LETTERS 86, 231103 (2005)

Background-limited terahertz quantum-well photodetector

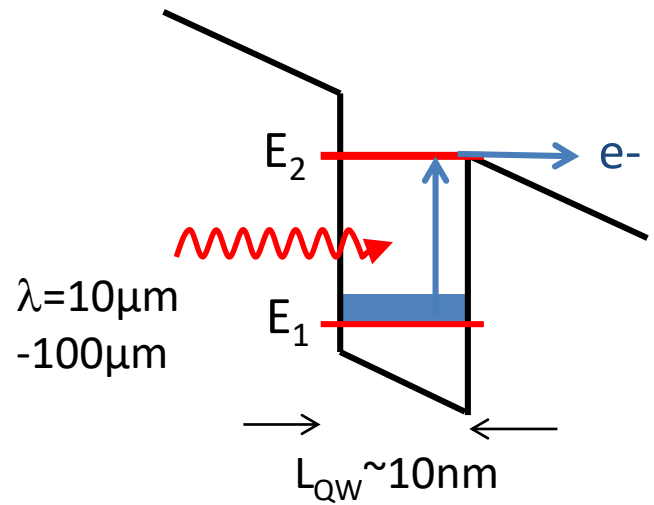
H. Luo,^{a)} H. C. Liu,^{b)} C. Y. Song, and Z. R. Wasilewski

Institute for Microstructural Sciences, National Research Council, Ottawa K1A 0R6, Canada

GaAs/AlGaAs quantum wells



Main issues addressed

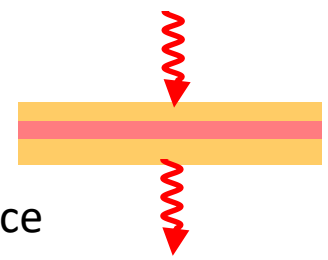


➔ Low quantum efficiency

2-3 % per well

➔ ISB selection rule

No absorption at normal incidence



➔ High dark current:

Low T operation to avoid the dark current



$\lambda=10\mu\text{m}, T \sim 70\text{K}$

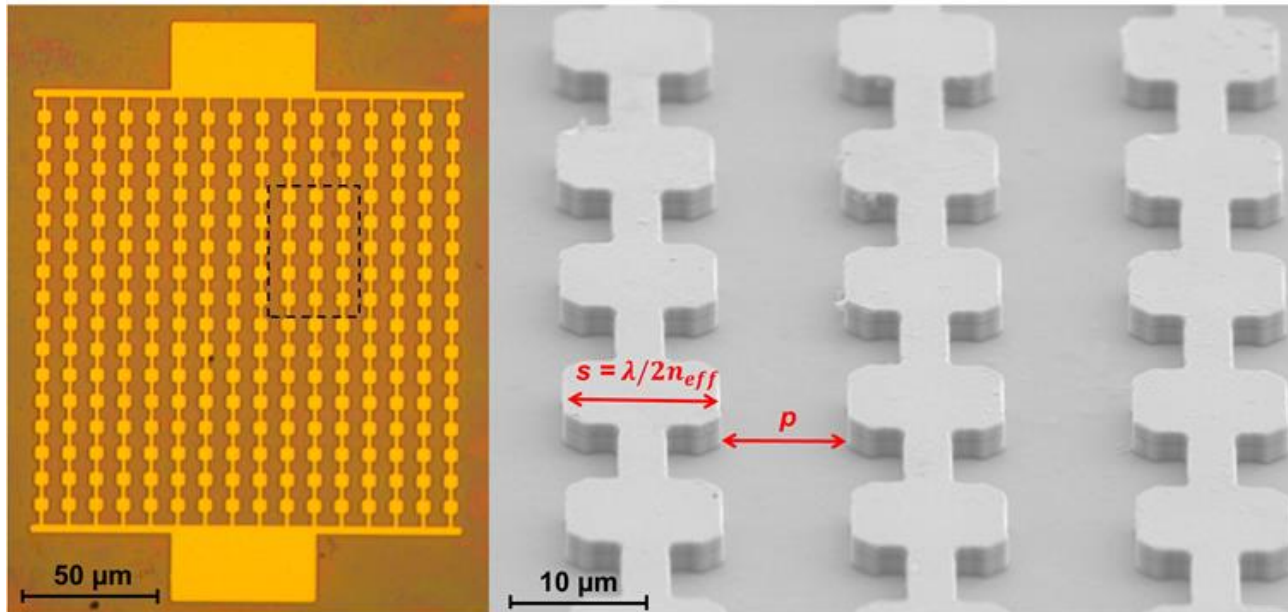
THz: $\lambda=100\mu\text{m}, T \sim 10\text{K} !$

Image: SOFRADIR website

Our approach: Patch antenna arrays

$p = 10 \mu\text{m}$

$s = 6, 7, 8, 9 \mu\text{m}$

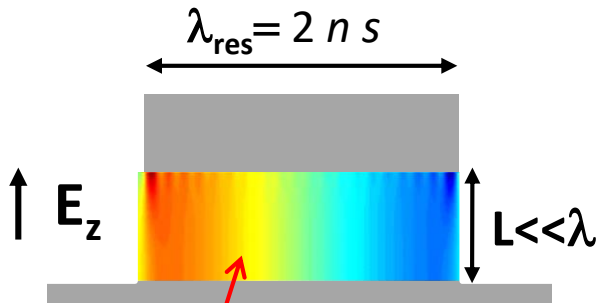
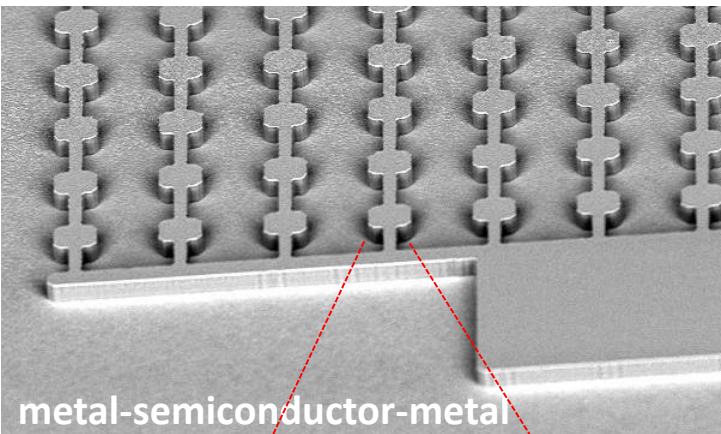


D. Palaferri et al.
APL. **106**, 161102 (2015)

Patch-antenna coupled microcavities

Quantum efficiency

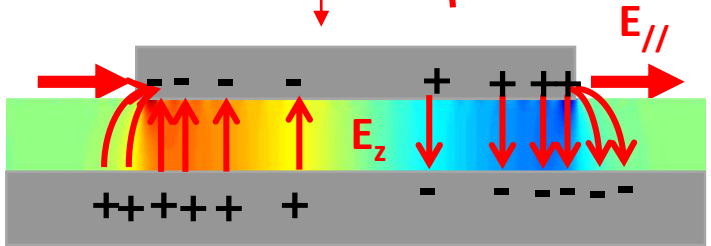
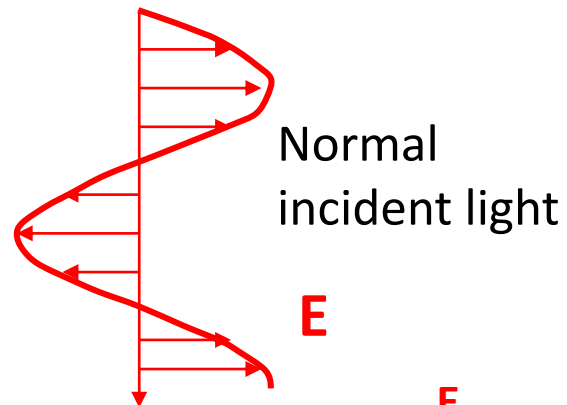
→ Microcavity



Standing wave
electromagnetic resonance

ISB selection rule

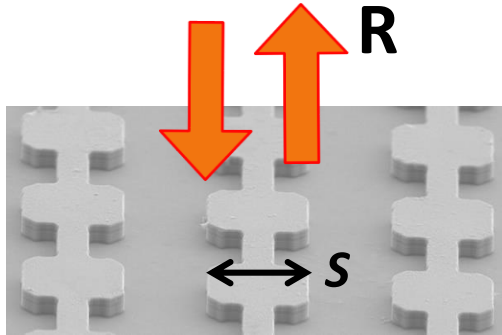
→ Quadrupole antenna



Capacity to rotate the polarization of the incident wave!

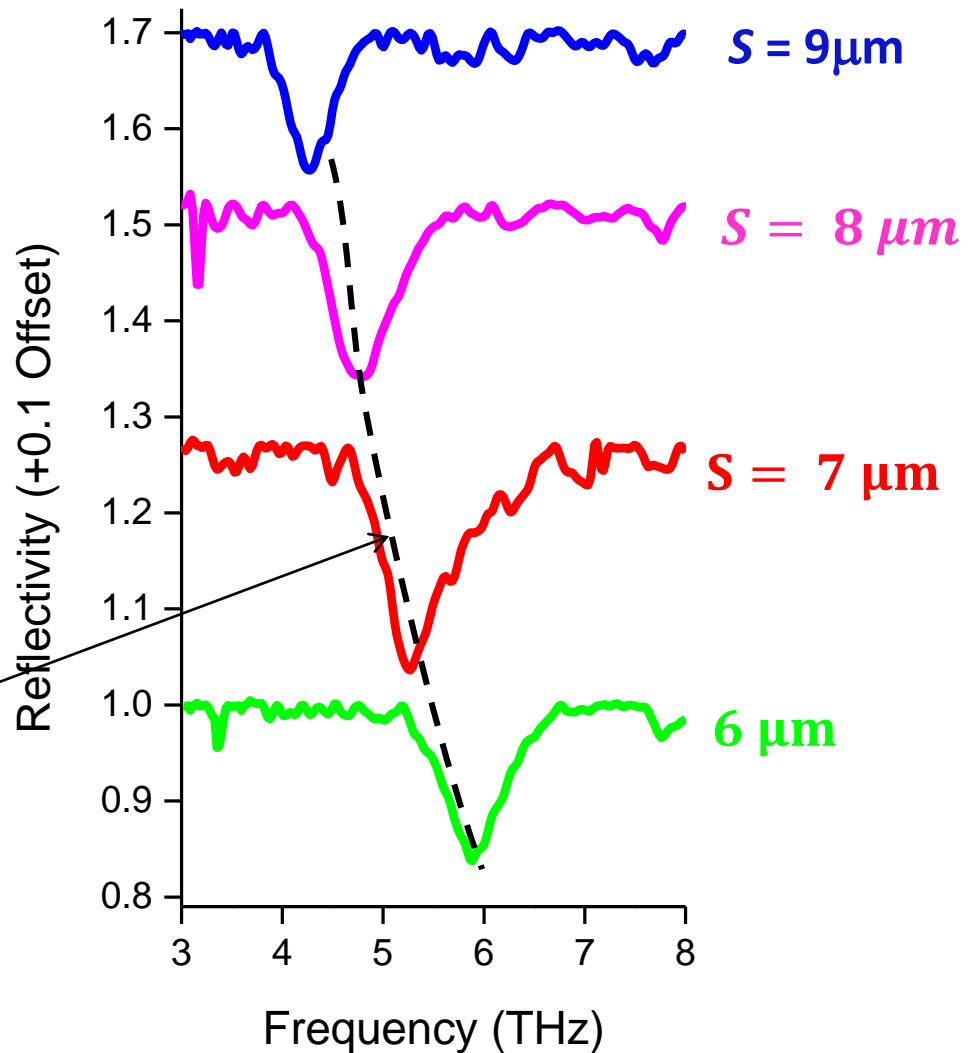
Balanis, C. A. *Antenna Theory* (John Wiley & Sons, 2005).

TeraHertz QWP: reflectivity measurements



Cavity mode tuning:

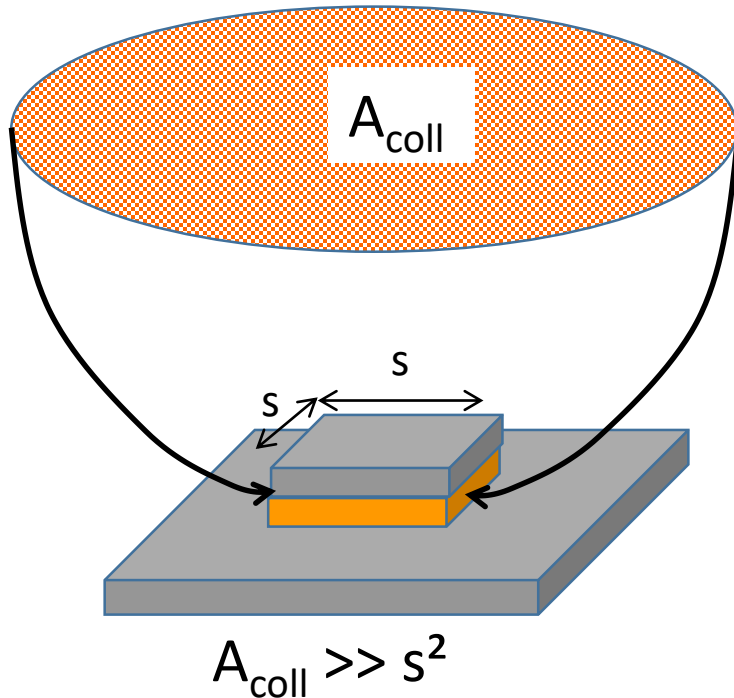
$$\lambda_{\text{res}} = 2 n s$$



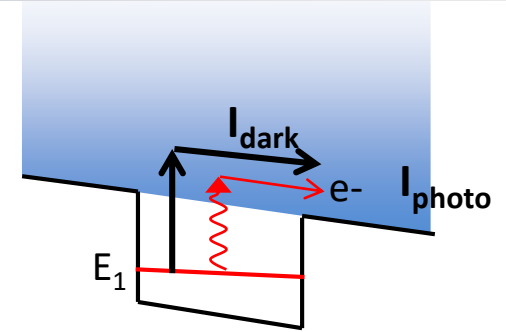
The benefits of antenna effects

High dark current

→ Antenna effect



Can collect photons from an area larger than the metal pad!



$$I_{\text{photo}} \sim A_{\text{coll}} \times \text{photon flux}$$

$$I_{\text{dark}} \sim s^2 \exp(-E_{\text{res}}/k_B T)$$

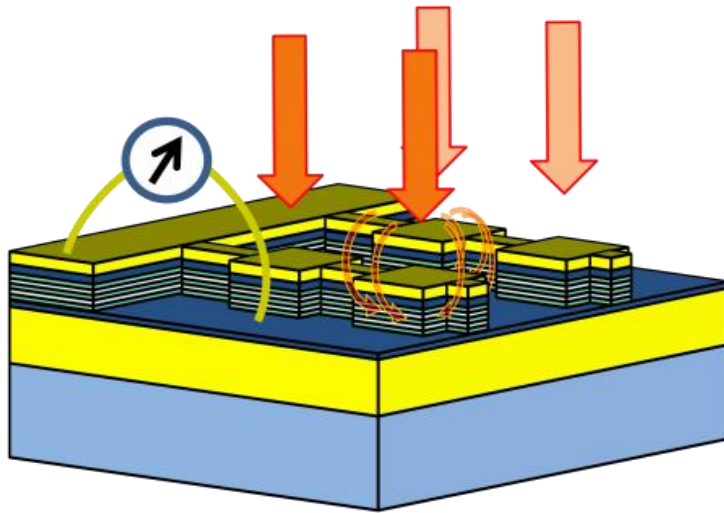
$$A_{\text{coll}}/s^2 \gg 1$$

Increased signal to noise ratio!

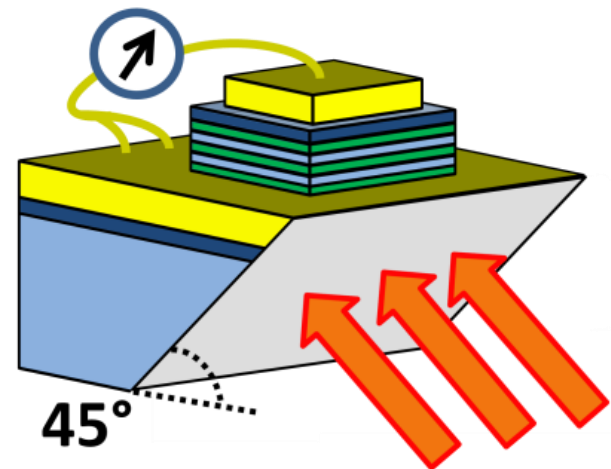
TeraHertz QWP: Comparative study

Two samples fabricated from the same wafer

Double-Metal geometry:
patch-antenna array

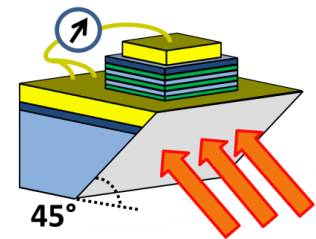
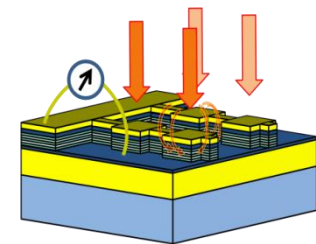
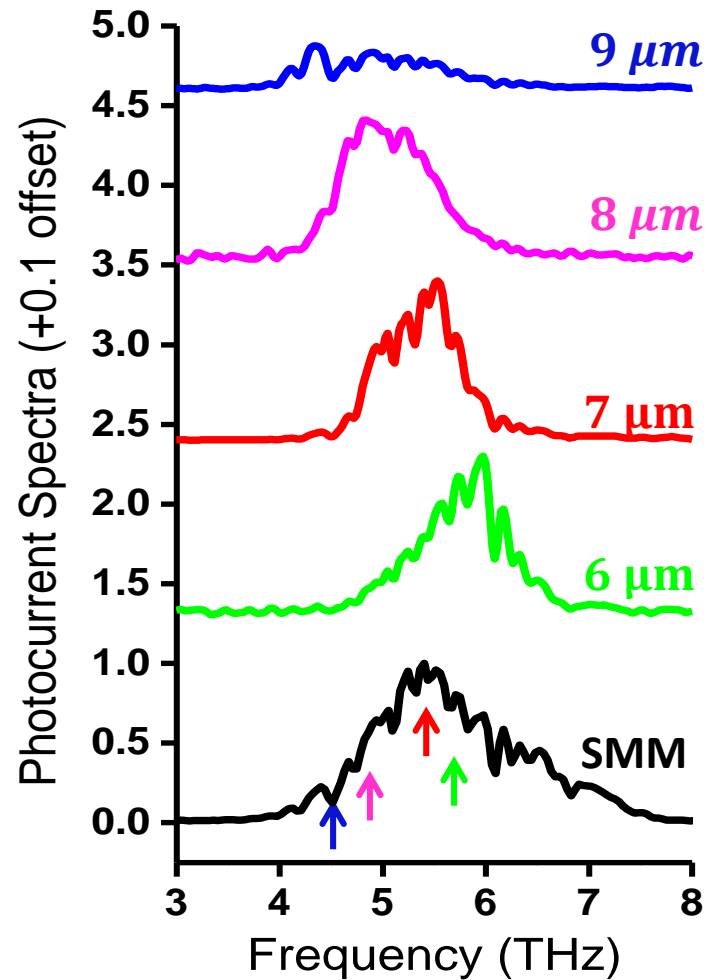
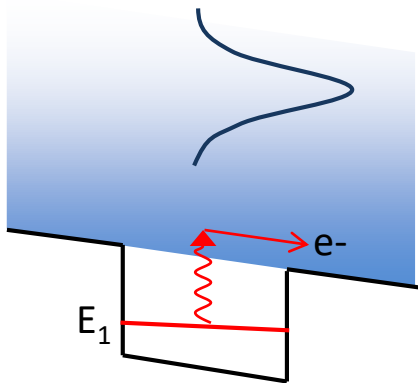


Single Metal Mesa
 $400 \times 400 \mu\text{m}^2$



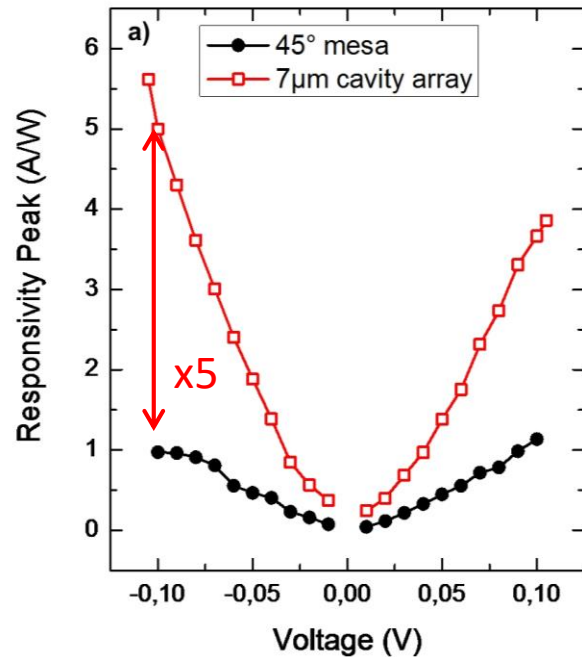
TeraHertz QWP: photo-current response

$T = 4\text{K}$

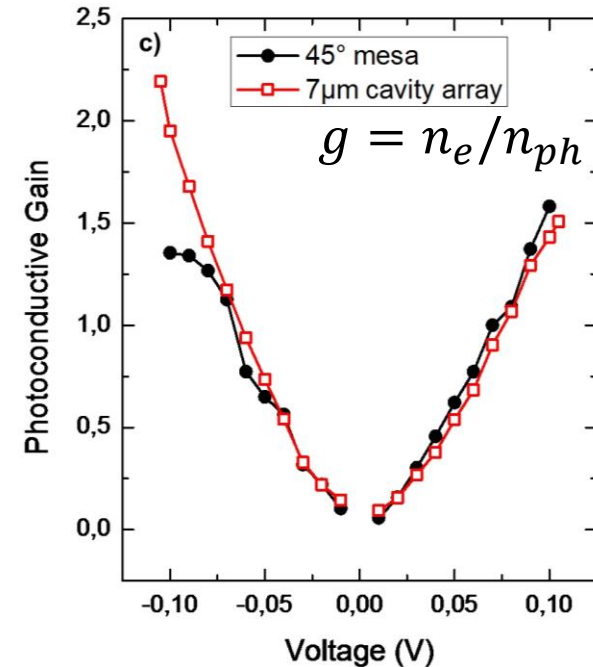
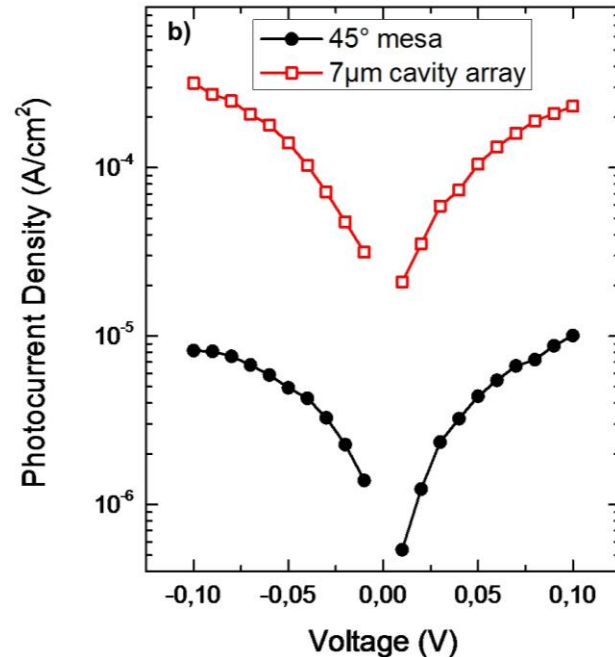


TeraHertz QWP: performance Analysis

Improved responsivity:
Microcavity



Higher photocurrent density
Antenna

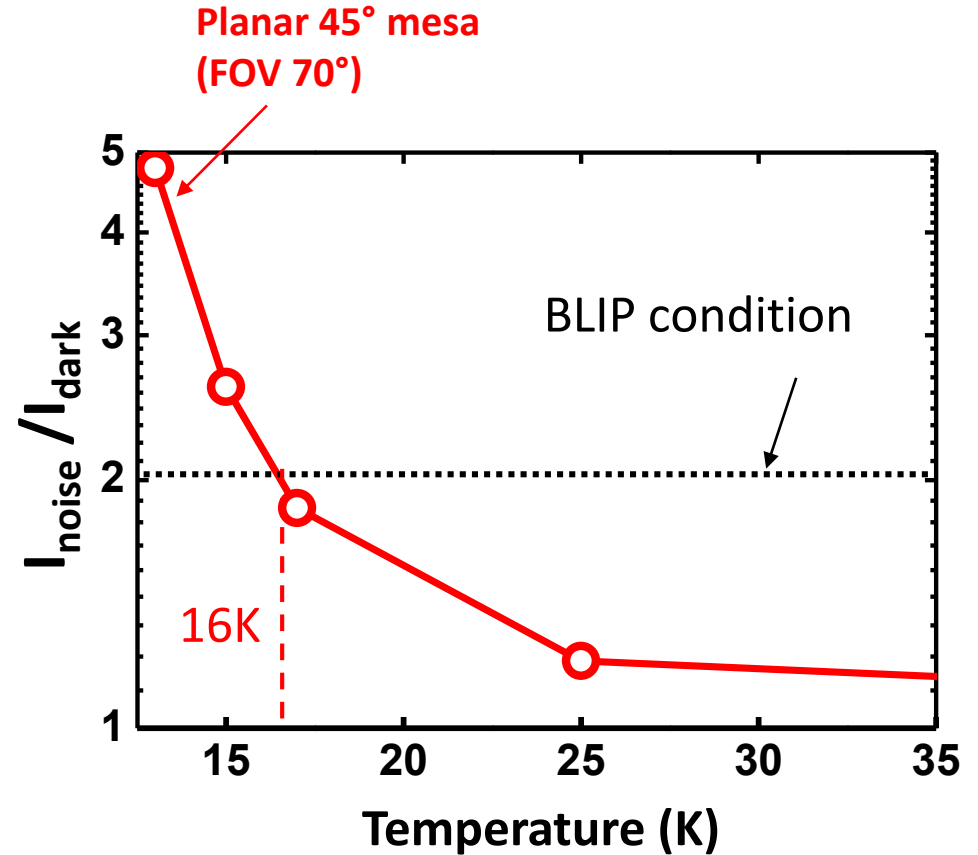
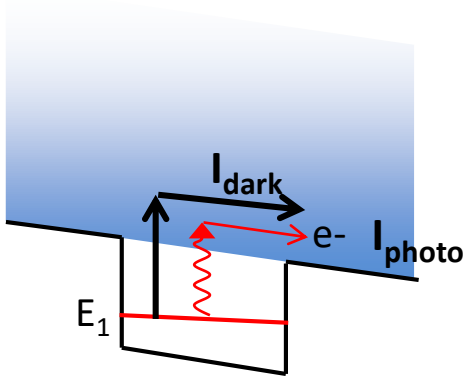


	D* BL	Optical NEP
7 μm – antenna QWIP	$1.7 \times 10^{11} \sqrt{Hz} \cdot cm/W$	0.18 pW/√Hz
doped Ge Bolometer (QMC)	$2.24 \times 10^{11} \sqrt{Hz} \cdot cm/W$	2.23 pW/√Hz

TeraHertz QWP: thermal performance

$$I_{\text{noise}} = I_{\text{dark}} + I_{\text{back}}$$

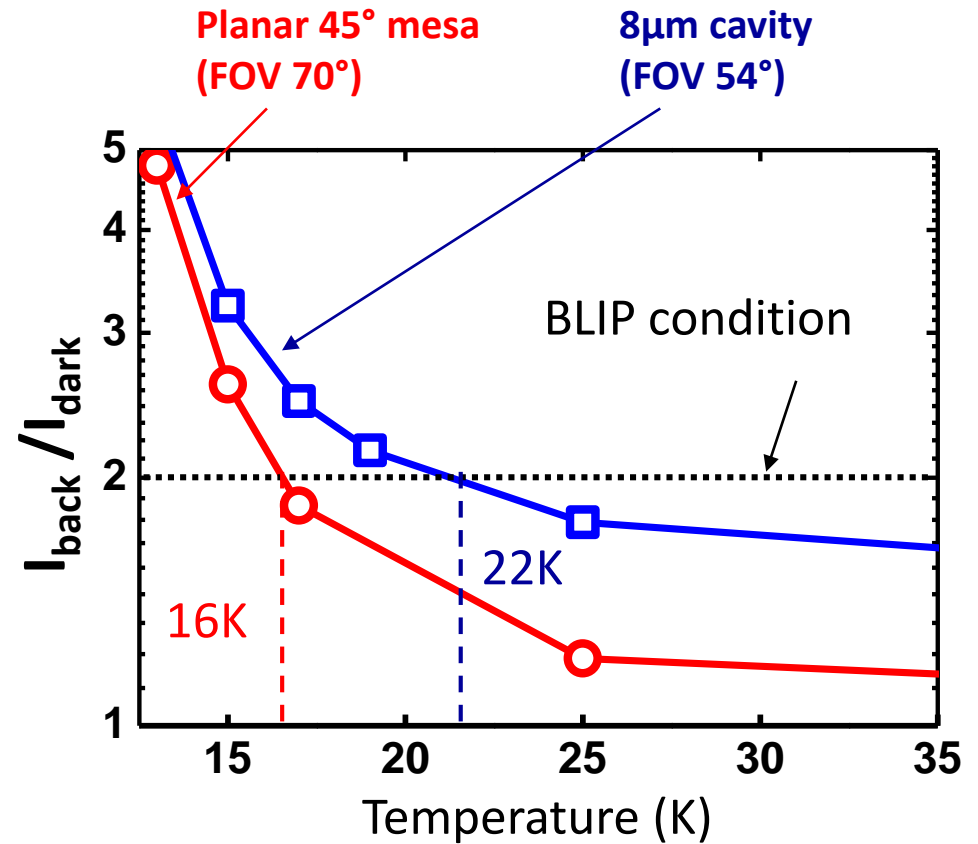
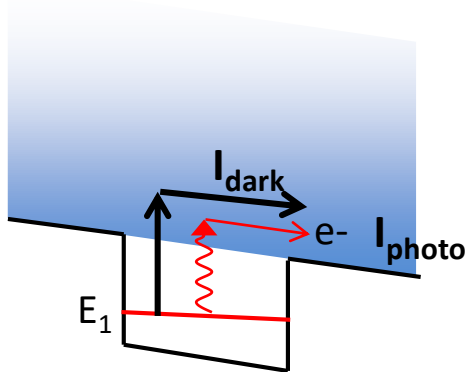
$$\text{BLIP condition: } I_{\text{noise}} = 2 I_{\text{dark}} (T_{\text{BLIP}})$$



TeraHertz QWP: thermal performance

$$I_{\text{noise}} = I_{\text{dark}} + I_{\text{back}}$$

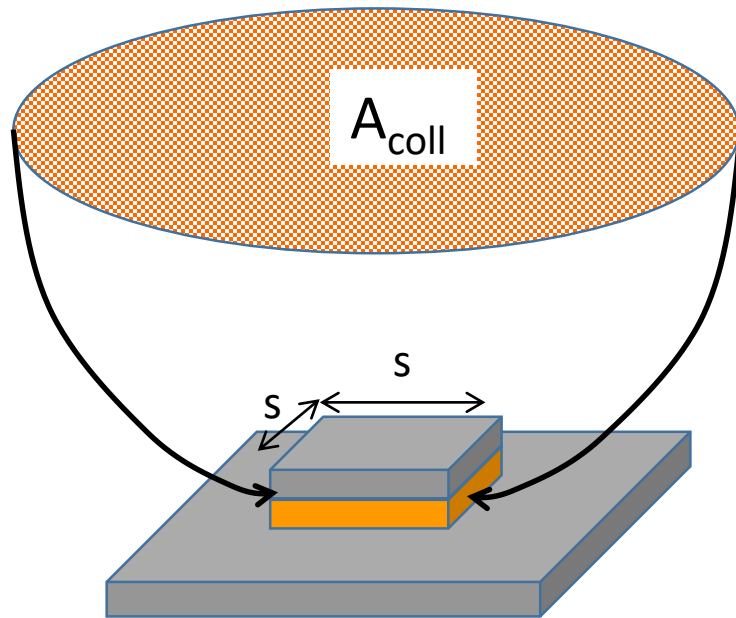
$$\text{BLIP condition: } I_{\text{noise}} = 2 I_{\text{dark}} (T_{\text{BLIP}})$$



Quantifying the temperature performance

How the inherent detector properties vary with the device architecture?

Knowing T_{BLIP}^0 (bare) what is T_{BLIP} (metamaterial) ?



$$A_{\text{coll}} \gg s^2$$

Bare detector performance

$$T_{BLIP} \approx \frac{T_{BLIP}^0}{1 - \frac{k_B T_{BLIP}^0}{E_{12}} (\ln F - k)}$$

Transition energy

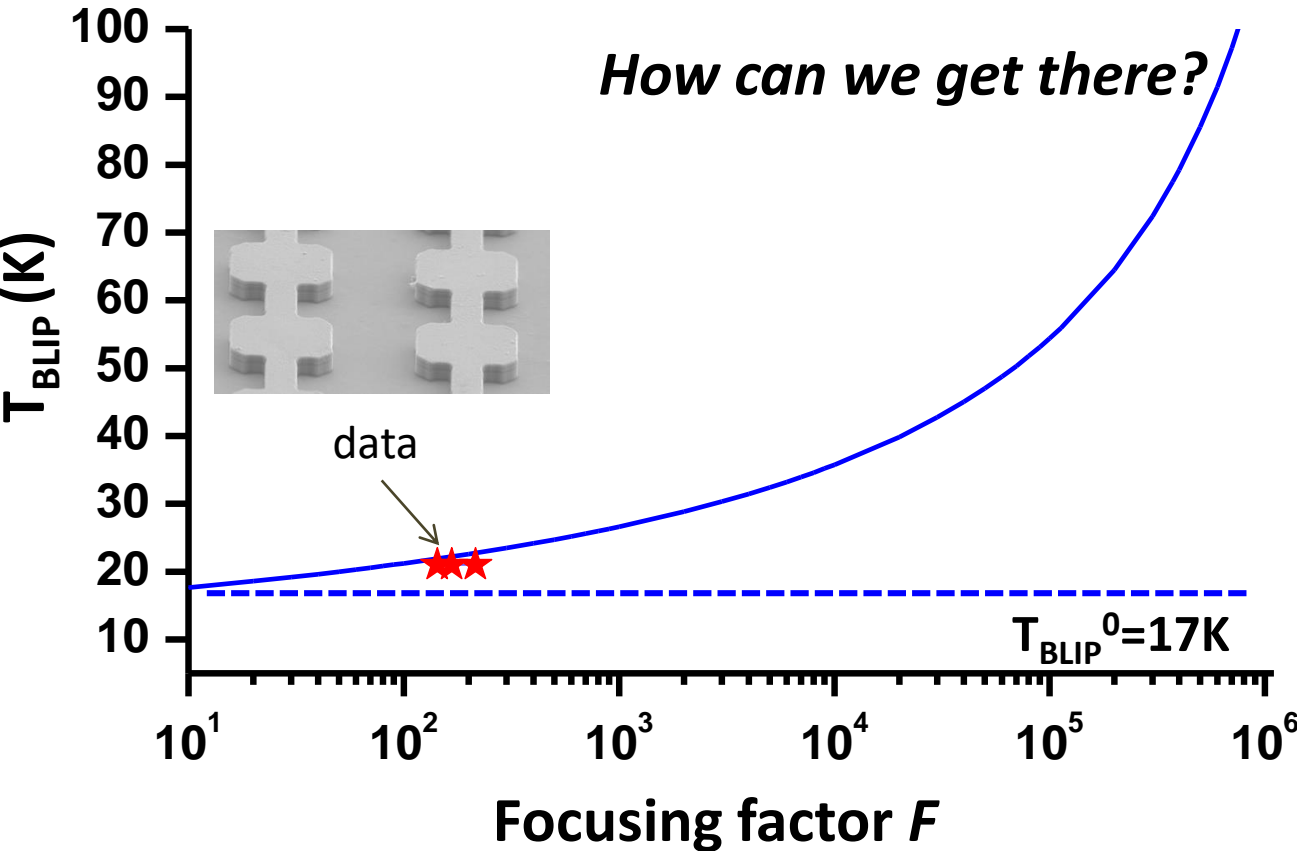
Focusing factor

$$F = \frac{\varepsilon |E_{\text{cav}}|^2}{|E_{\text{in}}|^2} = \frac{A_{\text{col}} \lambda_{\text{res}}}{V_{\text{cav}}} Q$$

Quality factor

$V_{\text{cav}} = s^2 L$

Focusing factor and temperature performance



Antenna effect

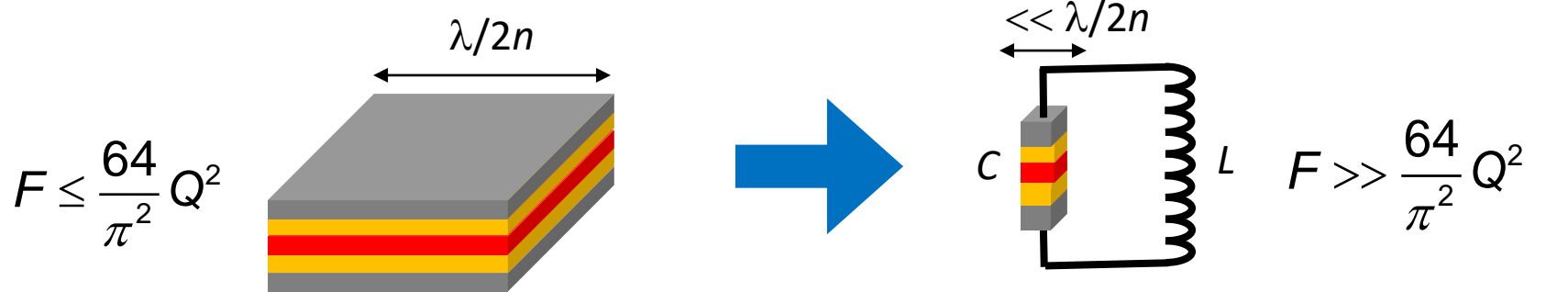
$$F = \frac{A_{col} \lambda_{res}}{V_{cav}} Q$$

Electromagnetic confinement

Going beyond the propagation limit

Moving from **optical macrocavities** to **electronic resonators**

Square patch Antenna



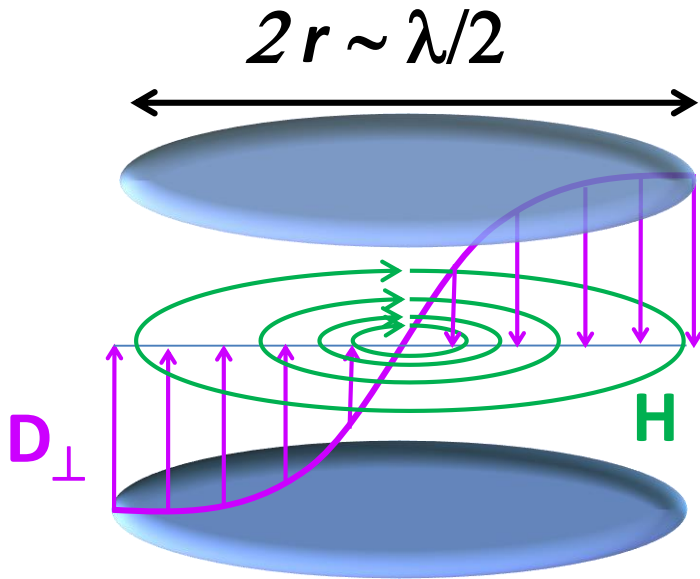
$v_{res} = \frac{c}{2n s}$

Optics

$\text{rot } \mathbf{H} = -\frac{\partial \mathbf{D}}{\partial t} + \mathbf{j}$

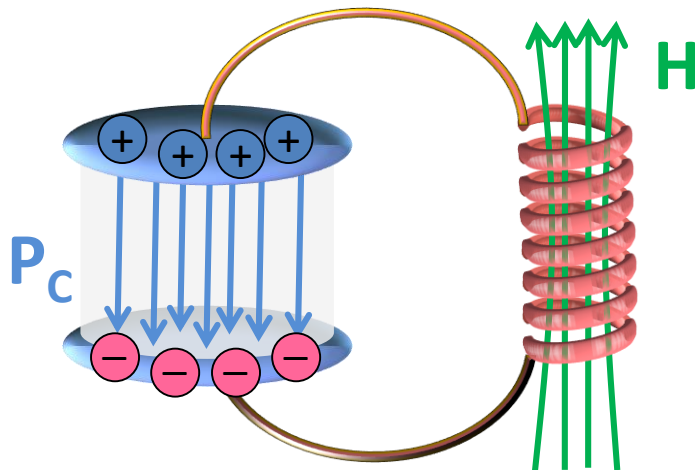
Electronics

$v_{res} = \frac{1}{2\pi \sqrt{LC}}$



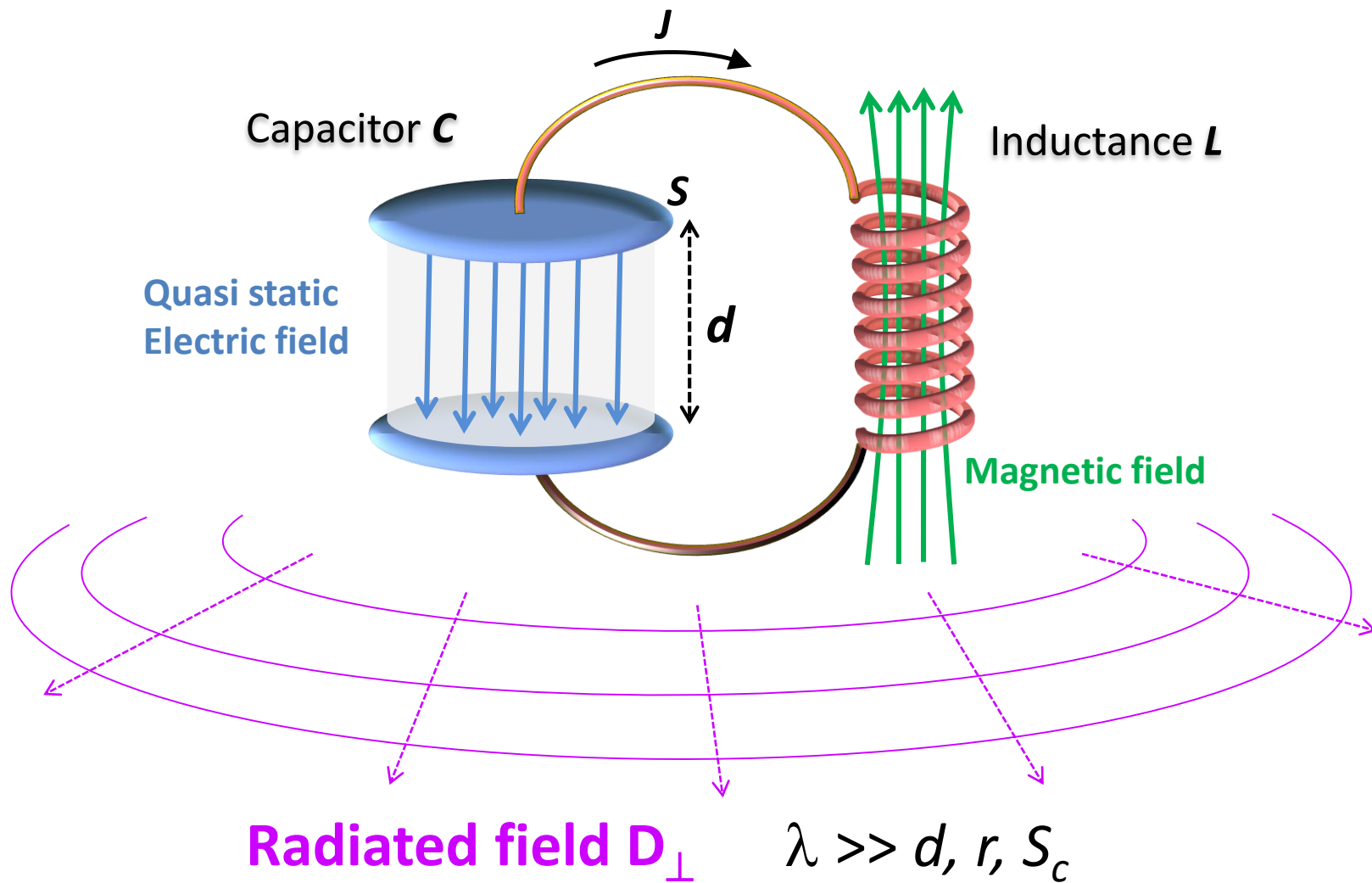
Optics

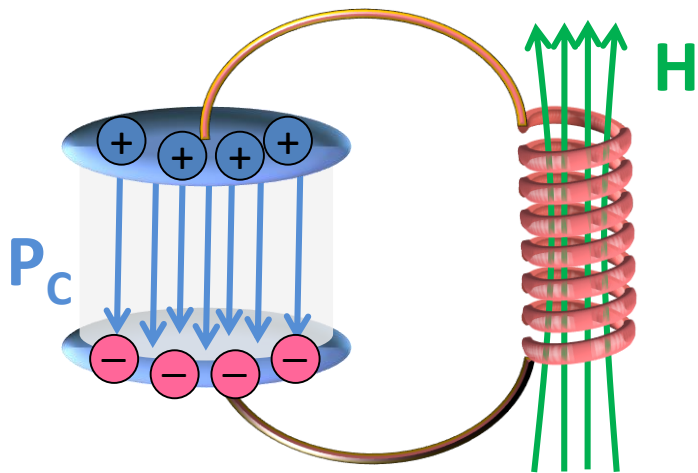
$$\int \frac{\mathbf{D}_{\perp}^2}{2\epsilon_0} d^3r + \int \frac{\mu_0 \mathbf{H}^2}{2} d^3r + \int \frac{\mathbf{P}_c^2}{2\epsilon_0 \epsilon} d^3r$$



Electronics

$$\int \frac{\mathbf{D}_{\perp}^2}{2\epsilon_0} d^3r + \int \frac{\mu_0 \mathbf{H}^2}{2} d^3r + \int \frac{\mathbf{P}_c^2}{2\epsilon_0 \epsilon} d^3r$$



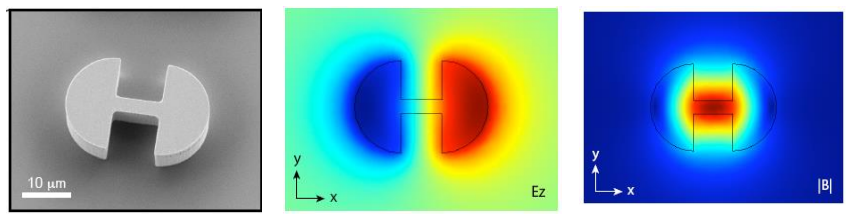


Electronics

$$\int \frac{\mathbf{D}^2}{2\epsilon_0} d^3r + \int \frac{\mu_0 \mathbf{H}^2}{2} d^3r + \int \frac{\mathbf{P}_C^2}{2\epsilon_0 \epsilon} d^3r$$

Going beyond the propagation limit

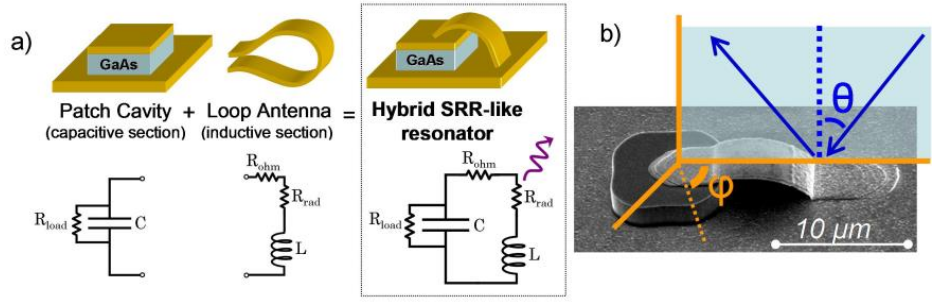
- LC-like patch cavities



C. Walther *et al.* Science (2010)

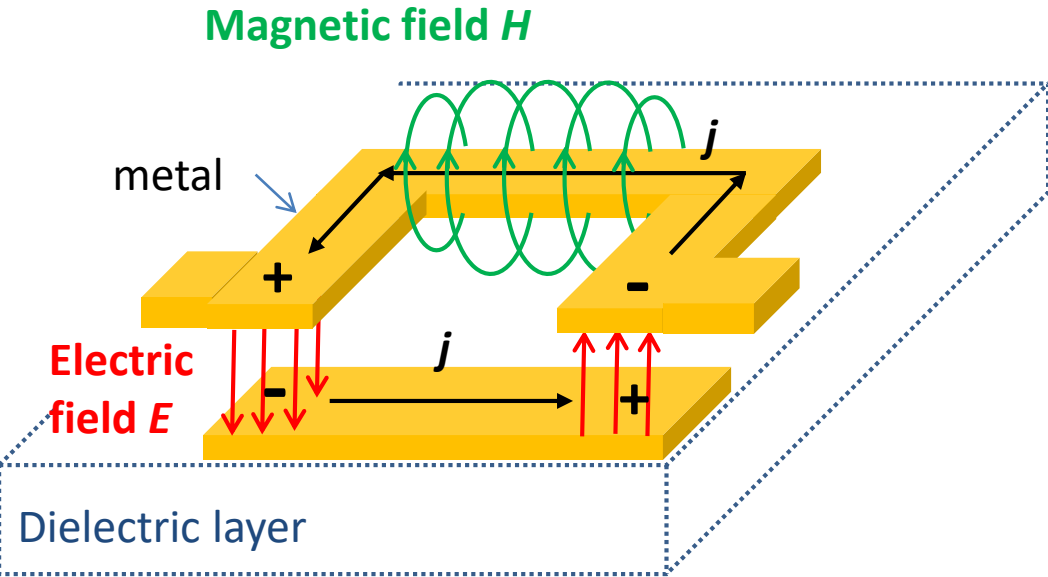
J. Faist's group (ETH Zurich)

- « Inverted » meta-materials



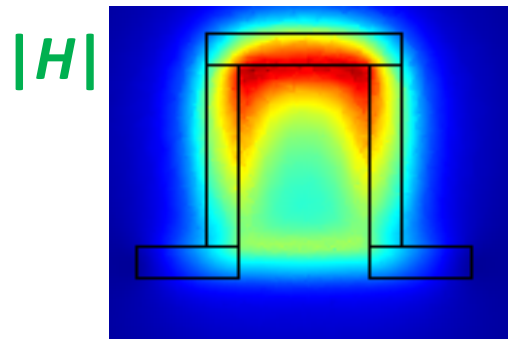
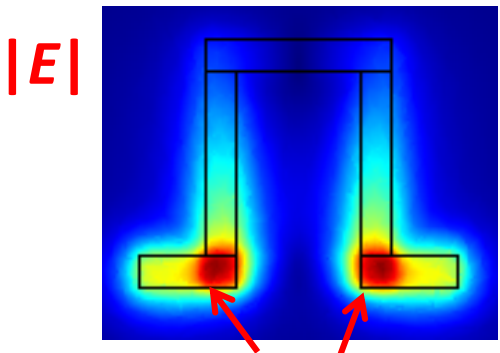
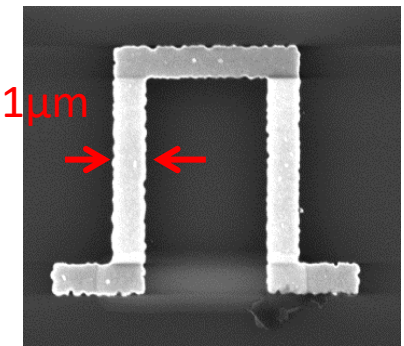
B. Paulillo *et al.*
 Opt. Express, **22**, 21302 (2014)

Metamaterial Detector



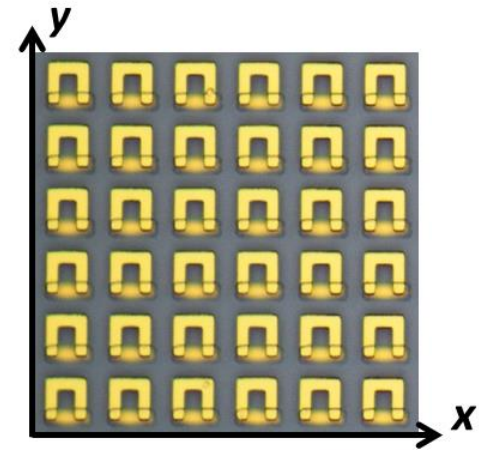
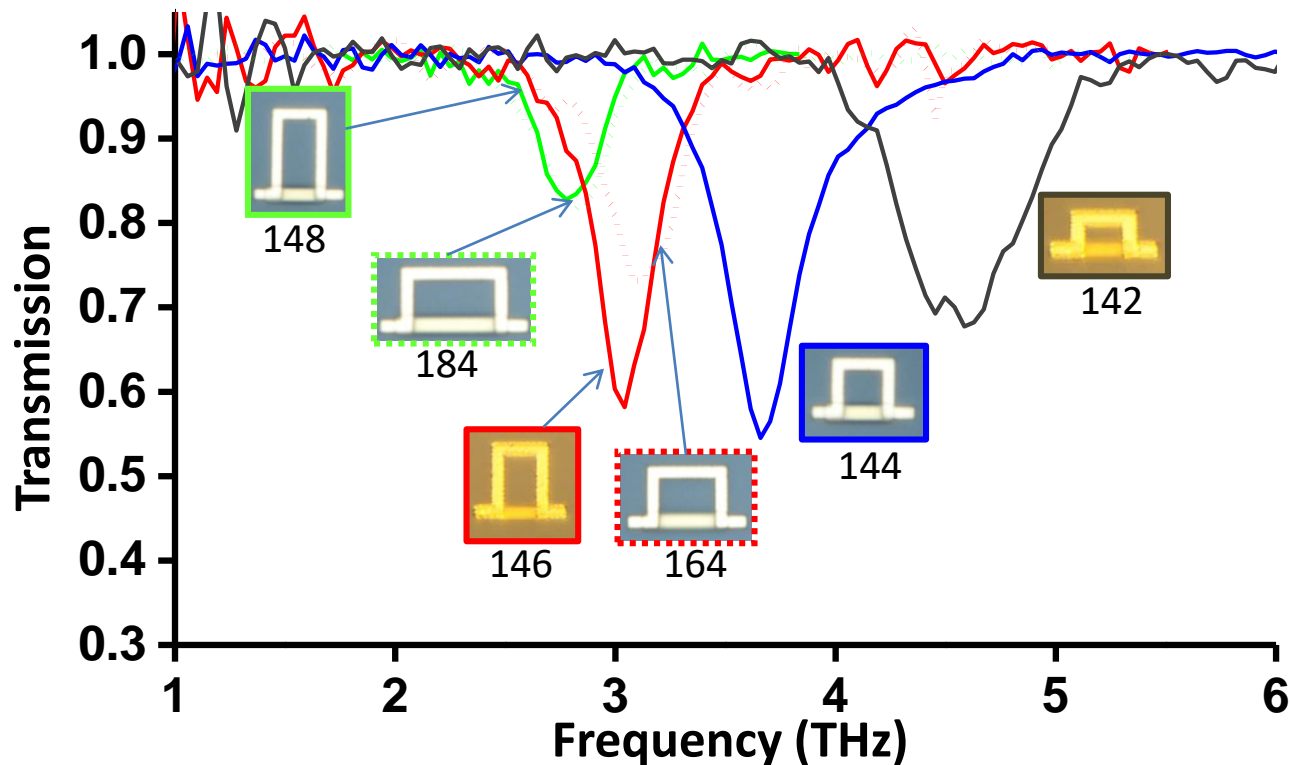
Advantages:

- Highly sub-wavelength confinement
- Propagation effects minimized
- Easy implementation of DC electrical pump/read-out



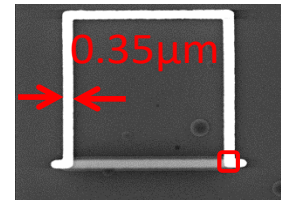
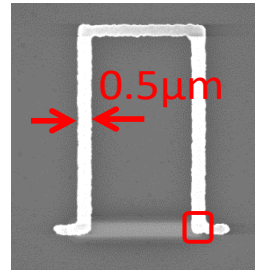
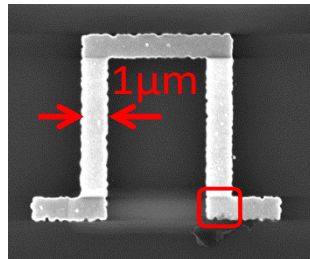
sub-wavelength capacitors

Transmission: tuning of the inductor size

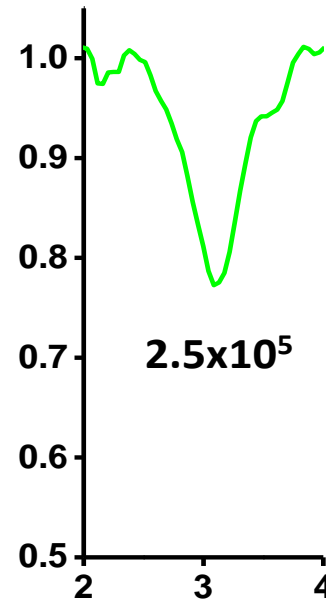
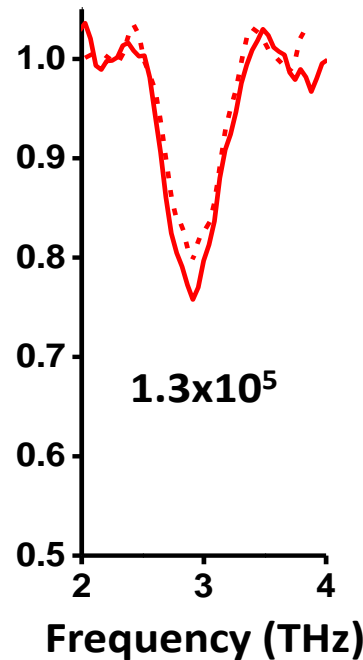
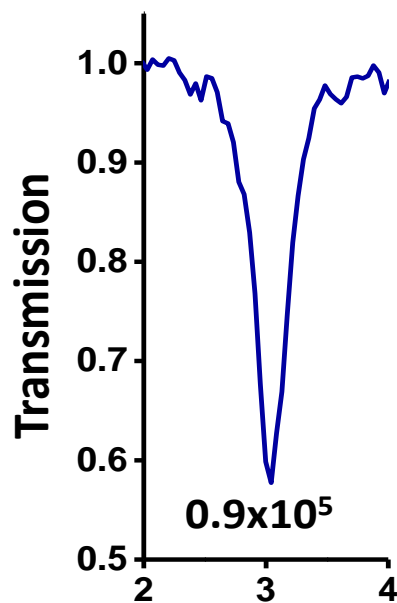


Tuning the capacitor

Smaller capacitors \rightarrow Smaller volume of interaction while keeping the resonance at 3THz



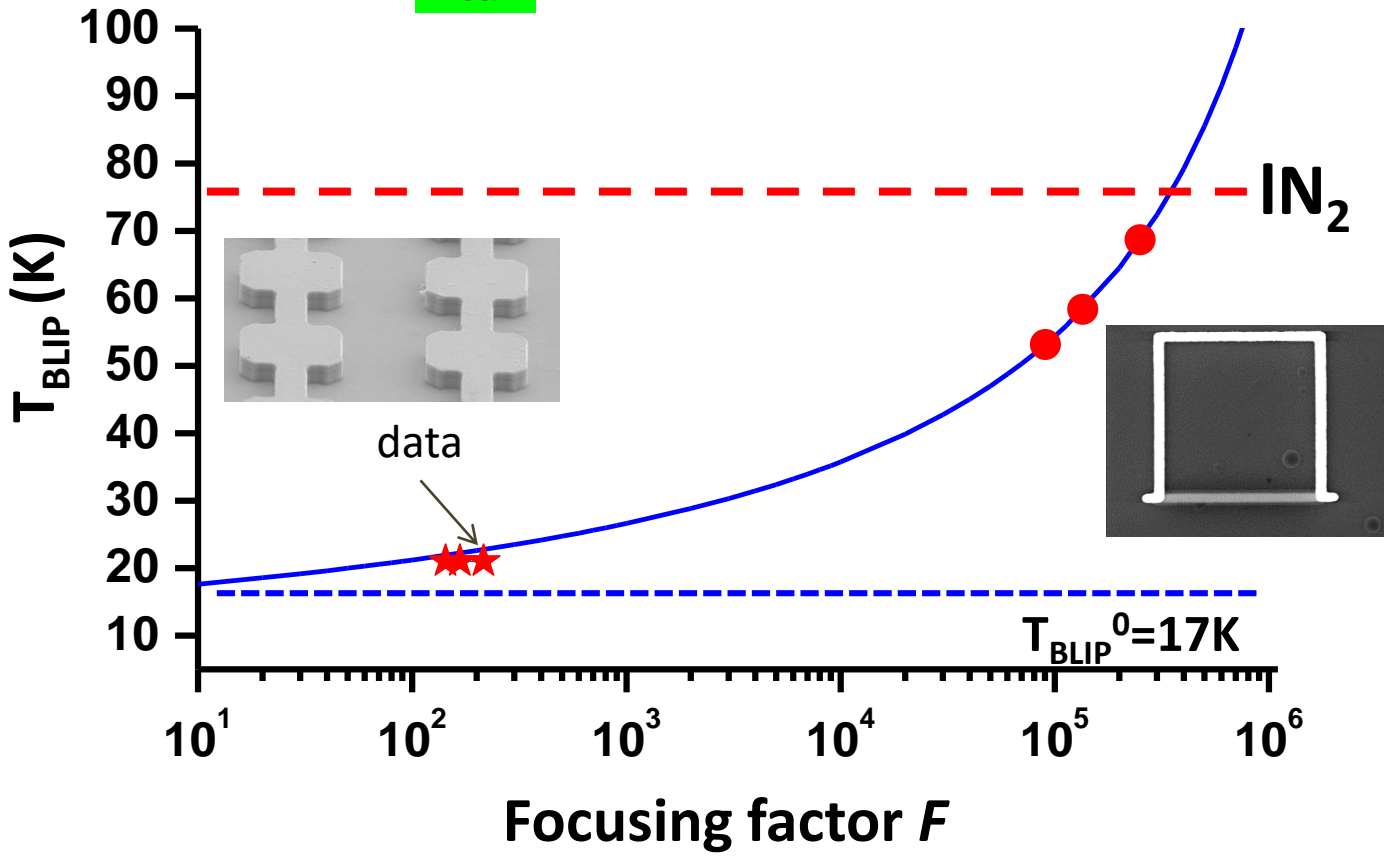
$$\omega_{LC} = \frac{1}{\sqrt{LC}}$$



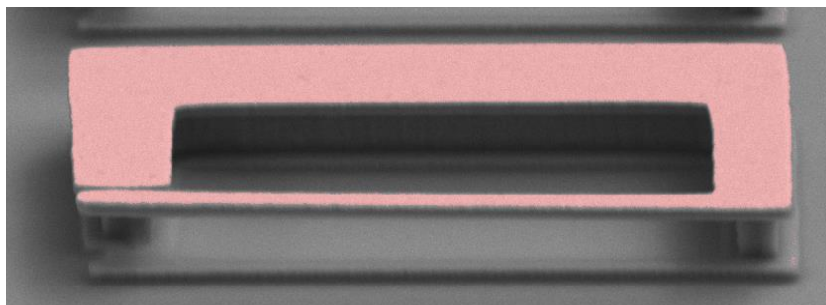
Resonant absorption in nanometers volumes

Focusing factor for LC structures

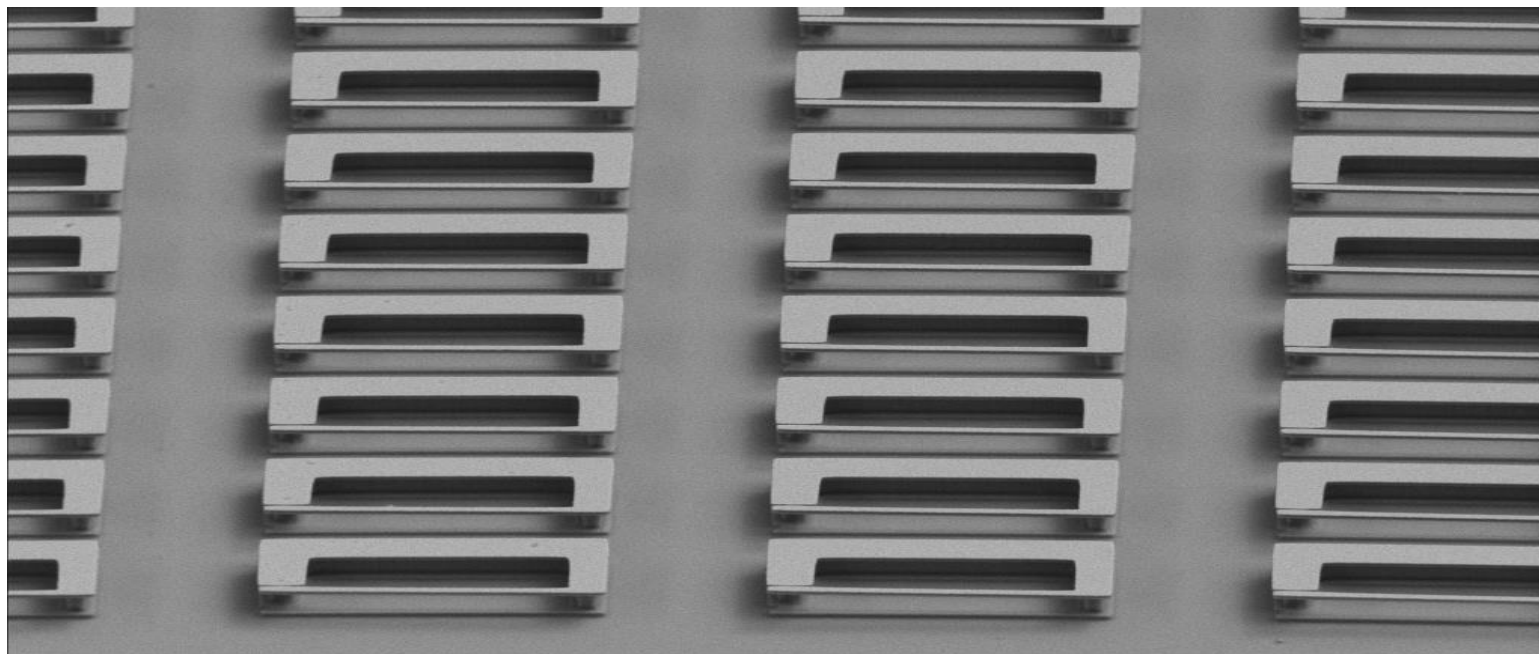
$$F = \frac{A_{col} \lambda_{res}}{V_{cav}} Q$$



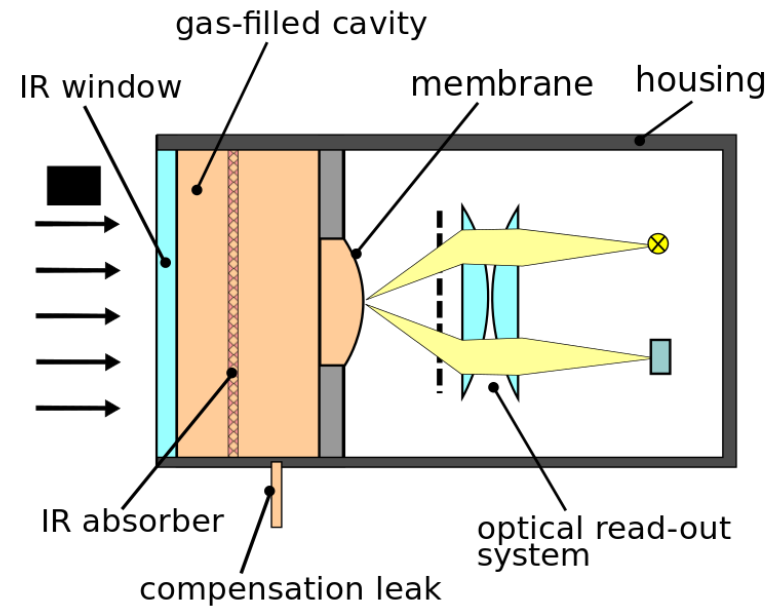
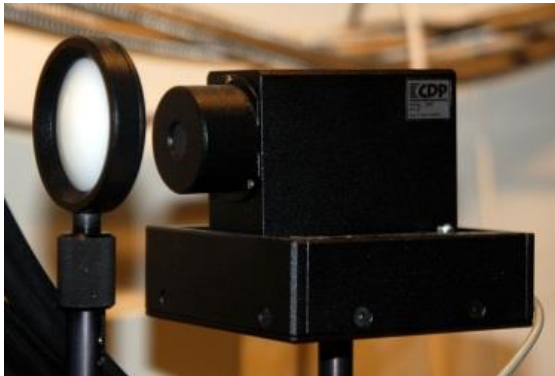
Liquid Nitrogen operation for quantum THz detectors !?



Optomechanical THz detection

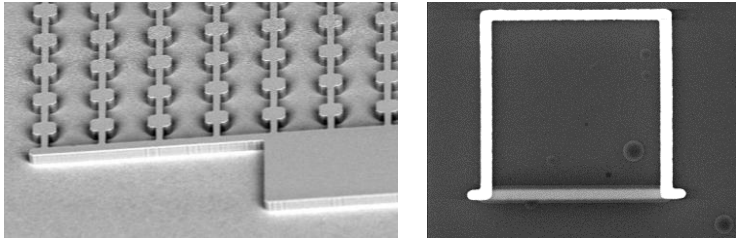


The Golay cell: an optomechanical device



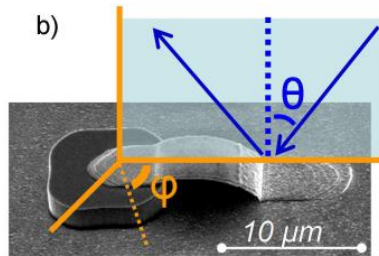
Metamaterials + optomechanics

THz metamaterials (for devices)

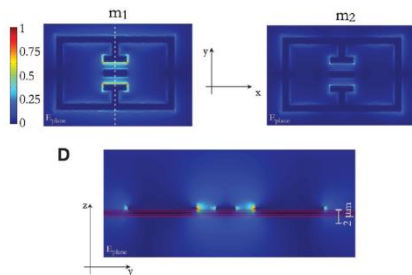


D. Palaferri et al., *APL*, **106**, 161102 (2015)

D. Palaferri et al., *New J. Phys.* **18** 113016 (2016)

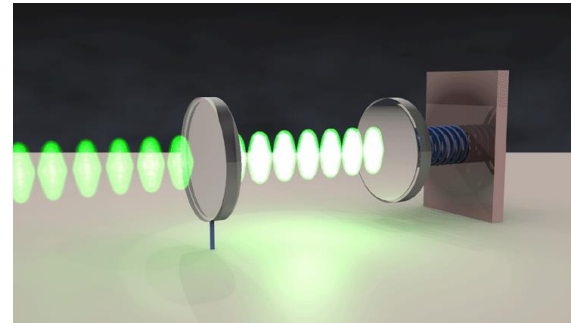


B. Paulillo et al. *Opt. Express*, **22**, 21302 (2014)

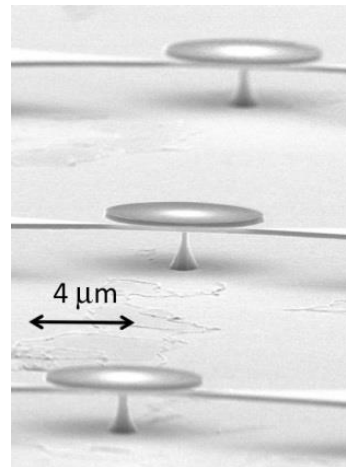


G. Scalari et al. *Science*, **335**, 1323 (2012)

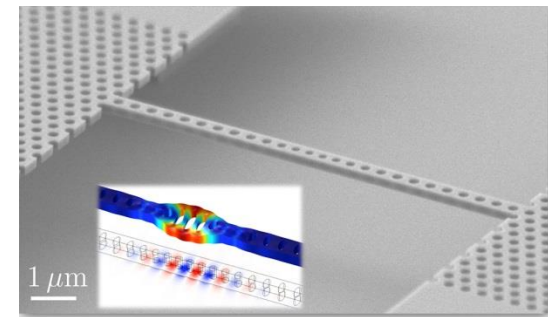
Optomechanics



I.Favero, and K. Karrai *Nature Phot.* (2009)

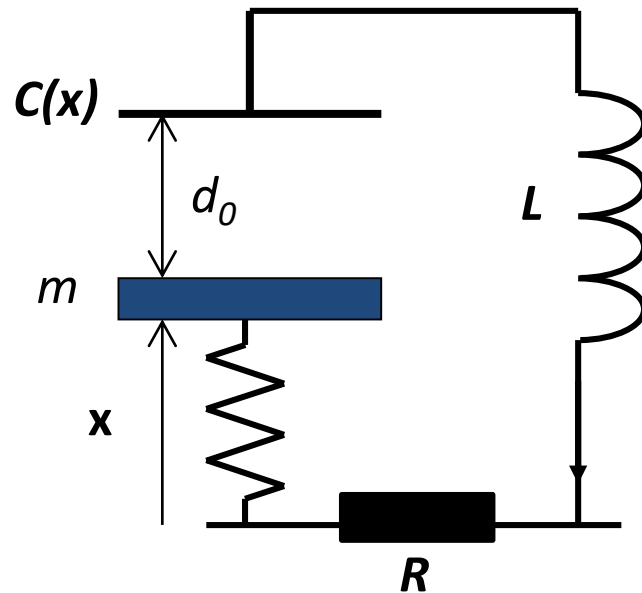


Courtesy I.Favero



C. Galland *et al.*,
Phys. Rev. Lett. **112**, 143602
(2014)

Optomechanics with THz metamaterials

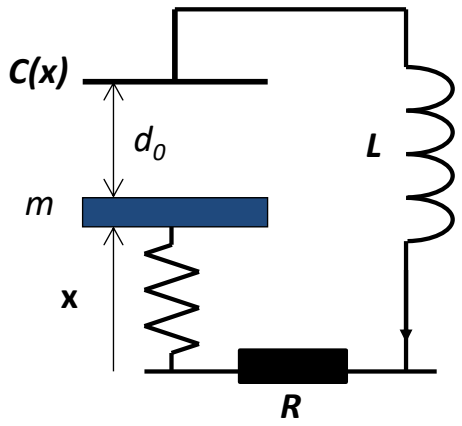


A device with 2 oscillators operating at 2 well distinct frequencies:

$$\omega_{LC} = \frac{1}{\sqrt{LC}} \approx 3THz$$

$$\omega_M = \sqrt{\frac{K}{m}} \approx 1MHz$$

Optomechanics with THz metamaterials



Dissipative term

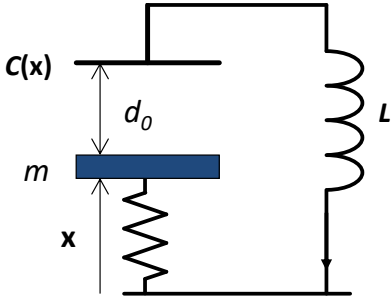
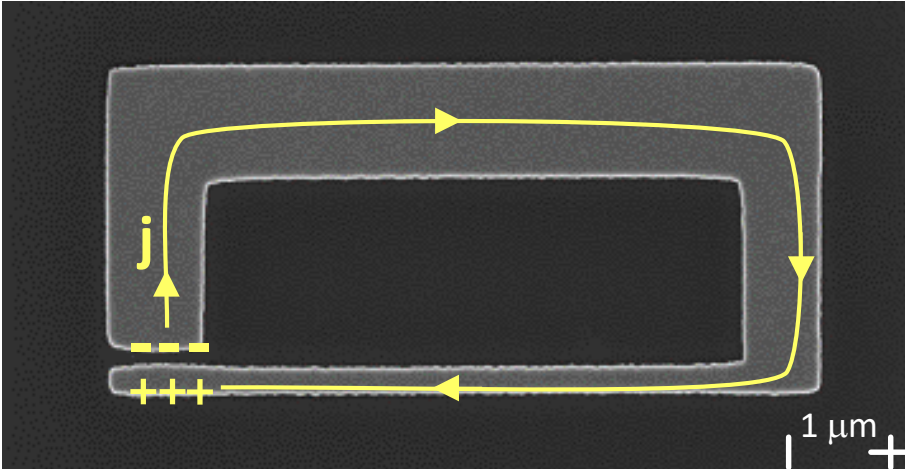
$$\frac{d^2 x}{dt^2} + \frac{\omega_M}{Q} \frac{dx}{dt} + \omega_M^2 x = \frac{W_{THZ}(t)}{m_{eff} d_0}$$

Cantilever mass
Capacitor spacing

THz energy coupled into the LC

Optomechanics with THz metamaterials

Split ring resonator with a movable arm

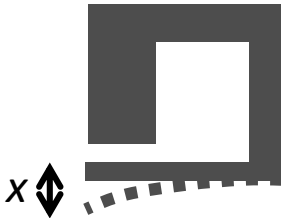
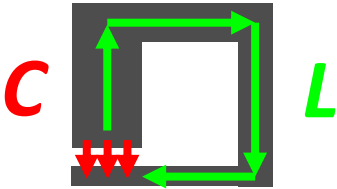


THz resonator

+

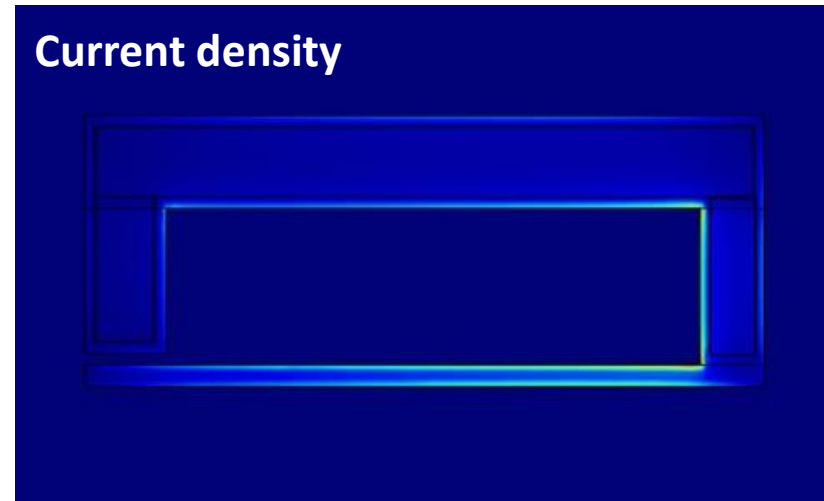
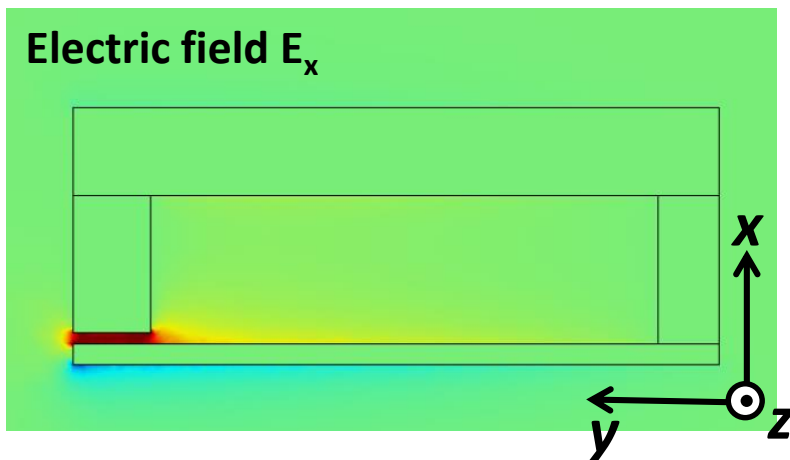
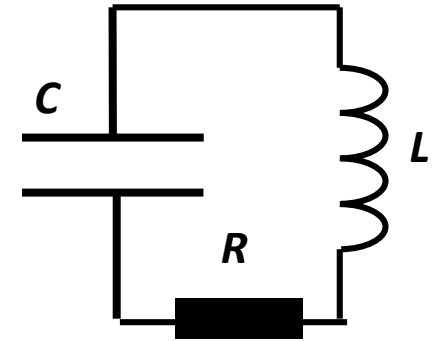
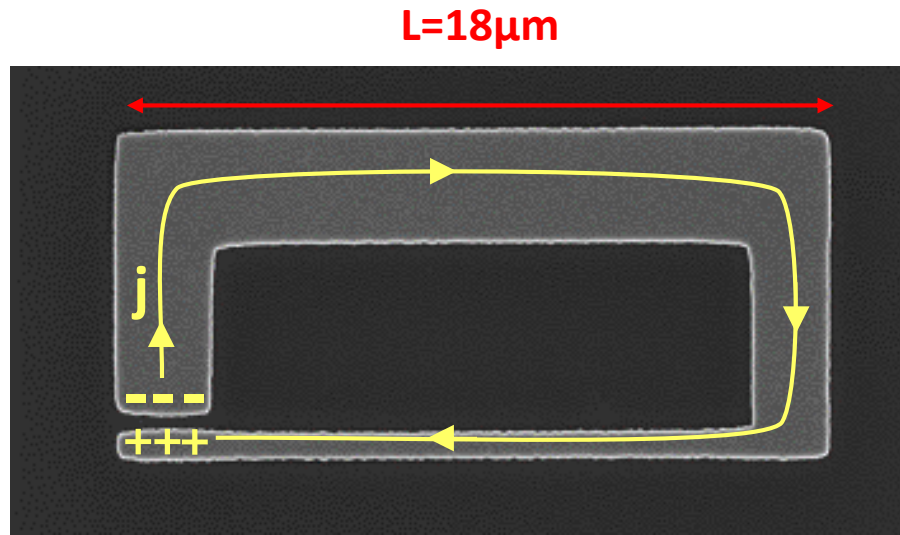
Mechanical resonator

$$f_{LC} = \frac{1}{2\pi\sqrt{LC}} = 3 \text{ THz}$$



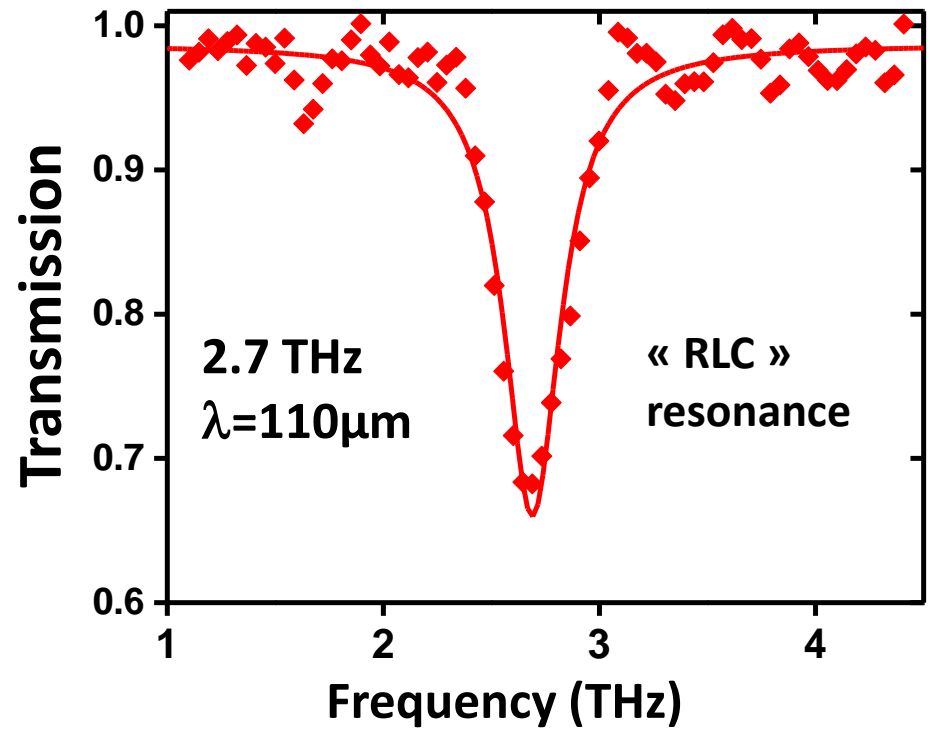
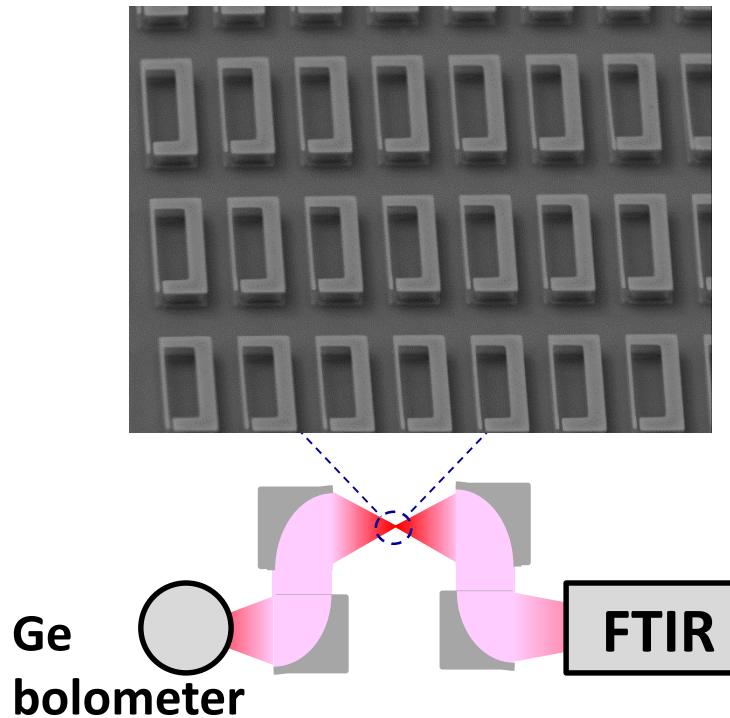
$$f_M = \frac{1}{2\pi} \sqrt{\frac{k}{m}} = 1 \text{ MHz}$$

THz optomechanical detector: optical part

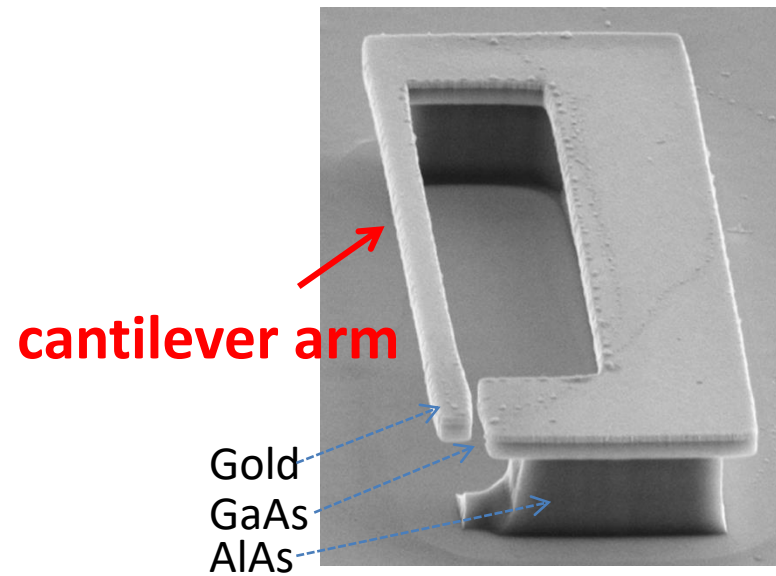


THz optomechanical detector: optical part

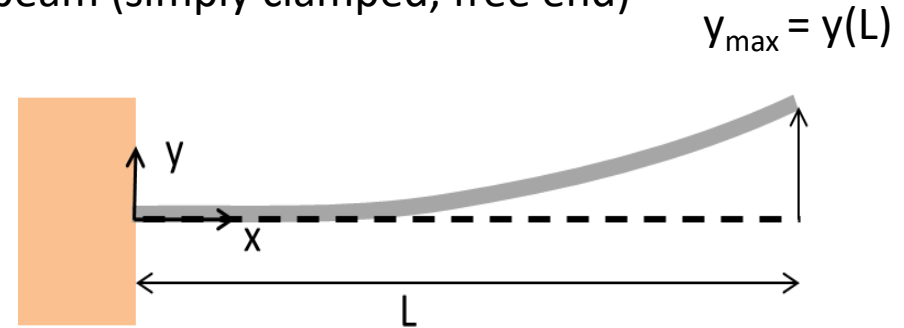
Probing in transmission FTIR



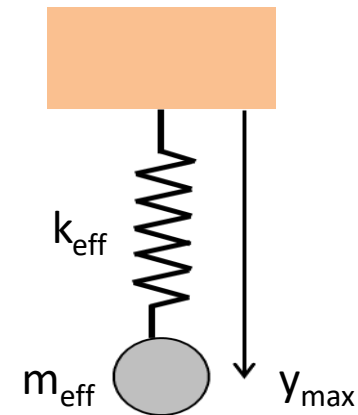
THz optomechanical detector: mechanical part



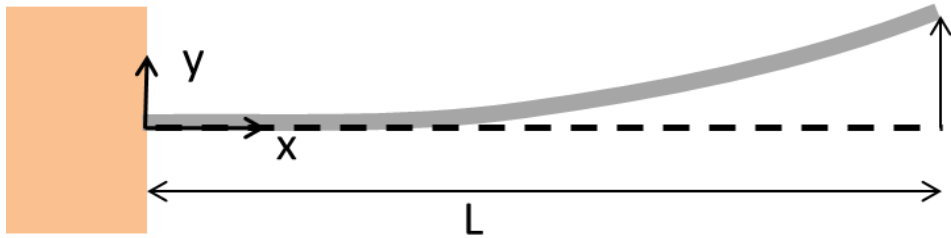
beam (simply clamped, free end)



equivalent 1D oscillator

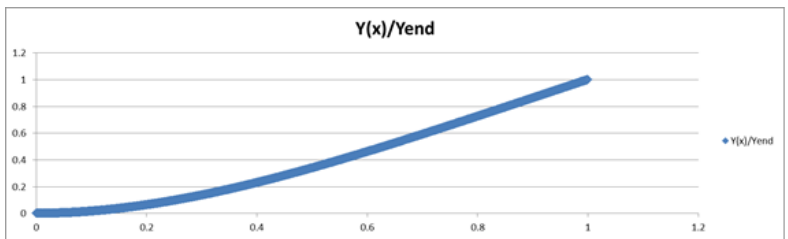


Equation of motion of a cantiliver

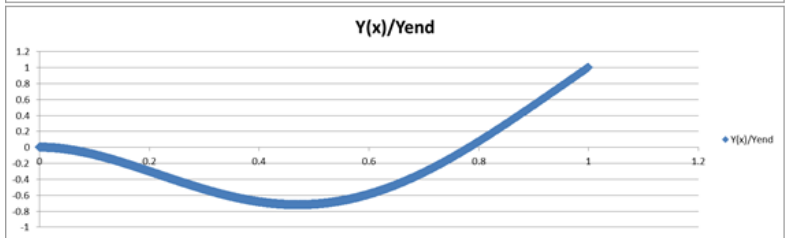


Eigen modes are solutions of the equation:
for appropriate boundary conditions.

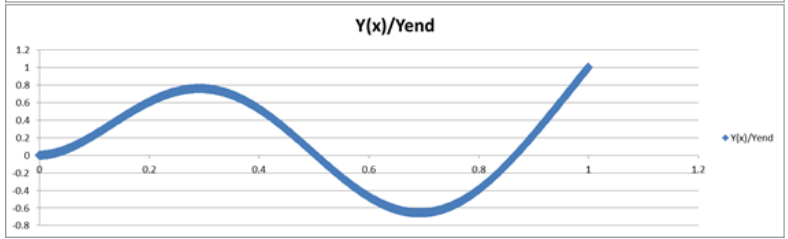
$$-EI \frac{\partial^4 y}{\partial x^4} = \rho \frac{\partial^2 y}{\partial t^2}$$



n=1

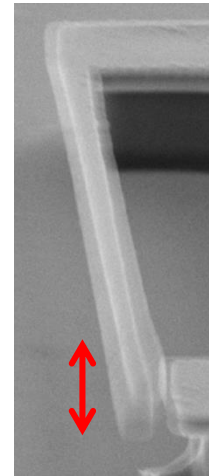
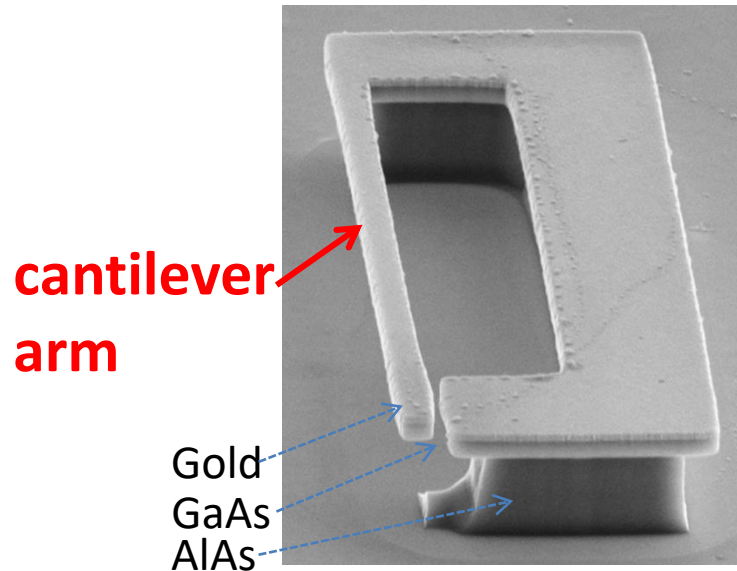


n=2

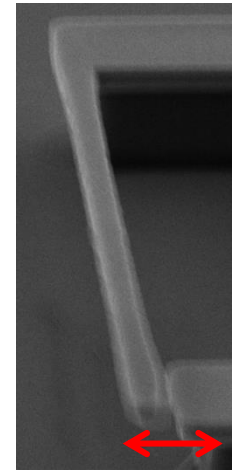


n=3

THz optomechanical detector: mechanical part



**955 kHz
out of -plane**



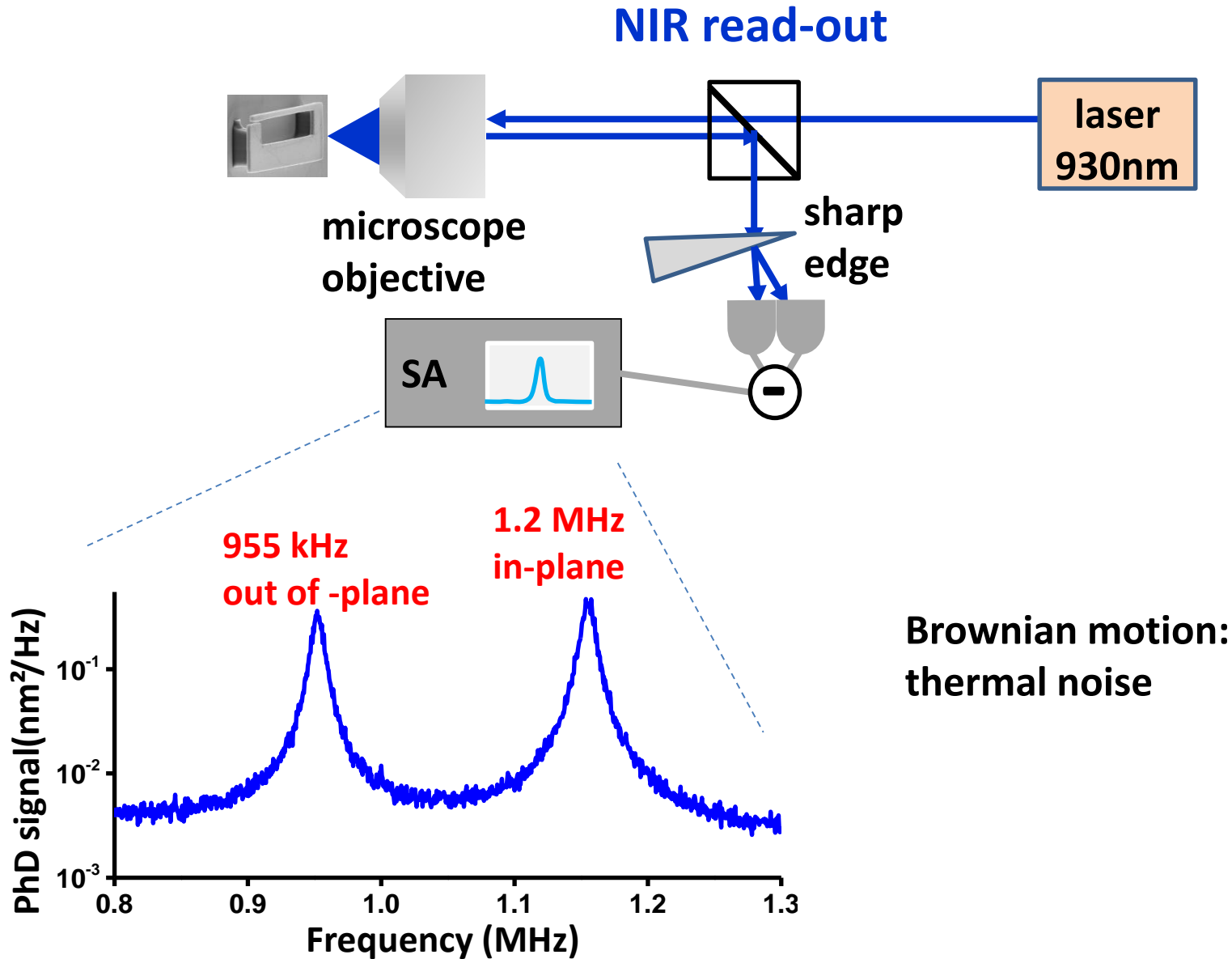
**1.2 MHz
in-plane**

$f_{1\perp} \sim \text{height}=475\text{nm}$ $f_{1\parallel} \sim \text{width}=581\text{nm}$

clamped bar:

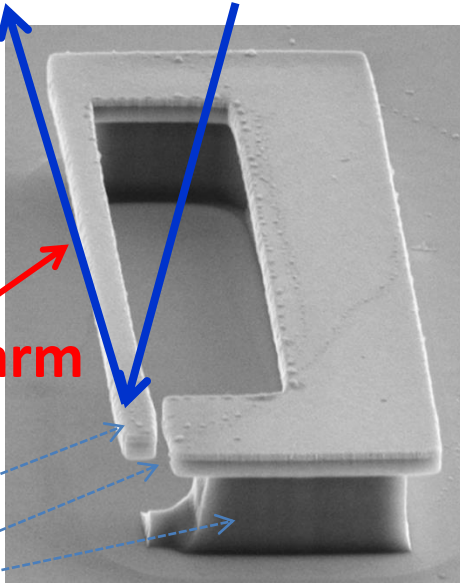
$$f_1 = 0.162 \frac{w}{L_c^2} \sqrt{\frac{Y}{\rho}} \quad L_c = 15\mu\text{m}$$

THz optomechanical detector: mechanical part



THz optomechanical detector: mechanical part

NIR read-out

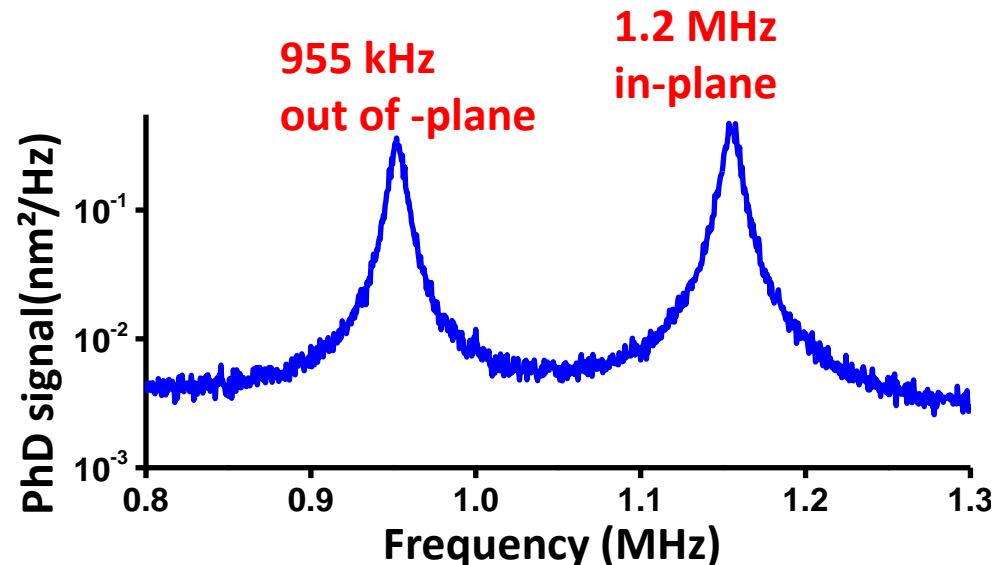


Brownian motion:
thermal noise

$$\frac{1}{2} m_{eff} \omega_m^2 \langle x^2 \rangle = \frac{1}{2} k_B T$$

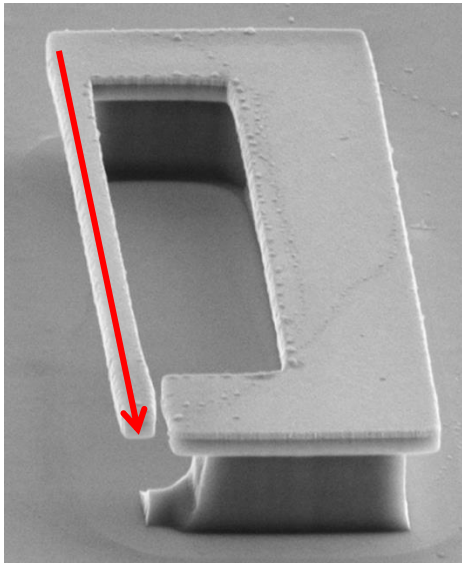
$$m_{eff} \sim 10 \text{ pg} \rightarrow \sqrt{\langle x^2 \rangle} \sim 1 \text{ \AA}$$

$$S_{xx}(f_m) = 2k_B T Q_m / m_{eff} \omega_m^3 = 0.33 \text{ pm}^2/\text{Hz}$$



High order modes

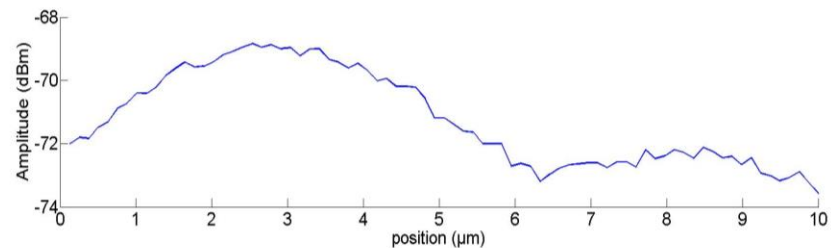
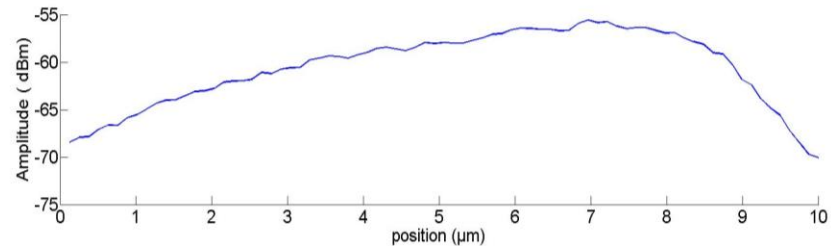
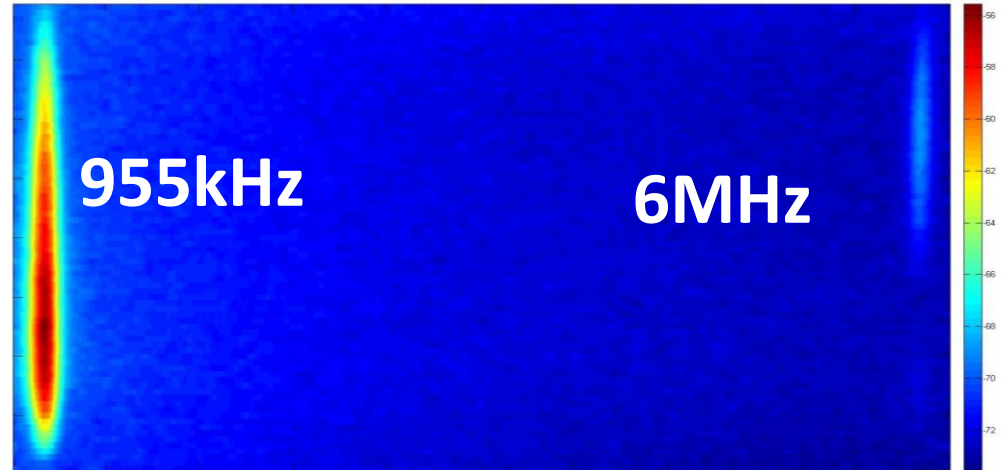
NIR read-out: higher order modes



$$f_n = 2.81 f_1 (n - 0.5)^2$$

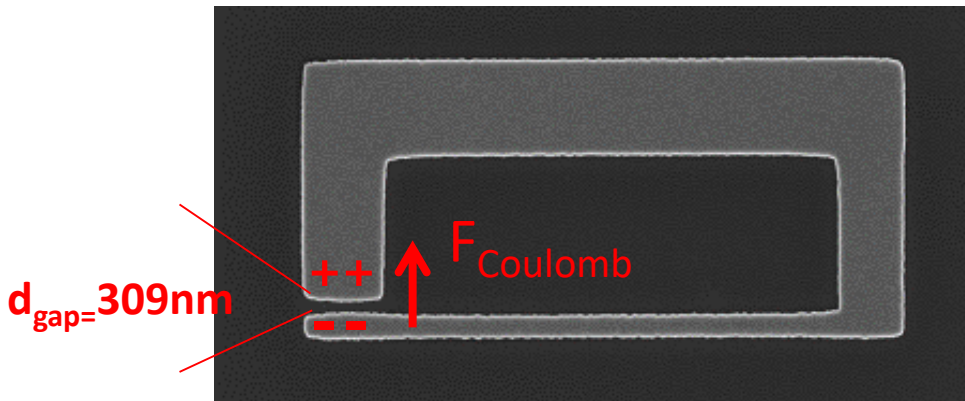
$$\frac{1}{2} m_{eff} \omega_m^2 \langle x^2 \rangle = \frac{1}{2} k_B T = const!$$

$$m_{eff} = 10 \text{ pg} = const$$



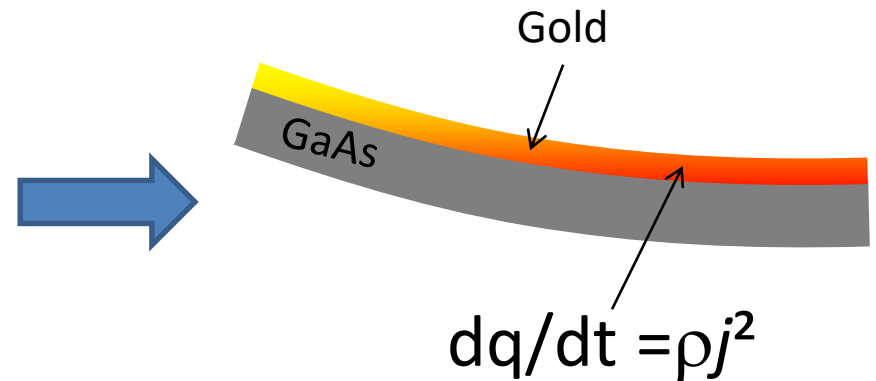
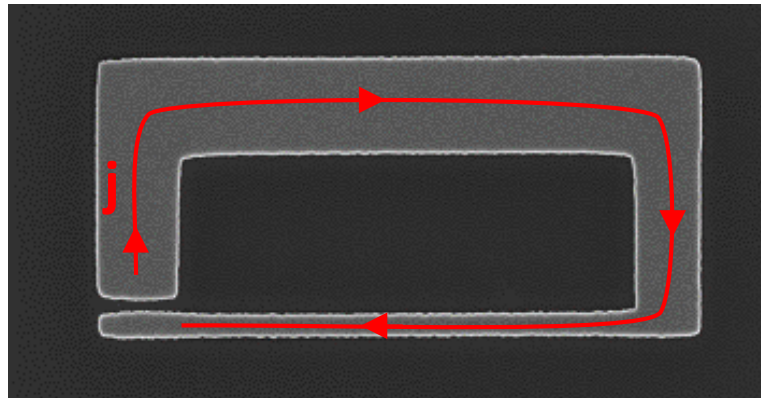
What kind of physical effects of the THz waves we can expect on this structure?

a. Electro-mechanical interaction: Coulomb force.



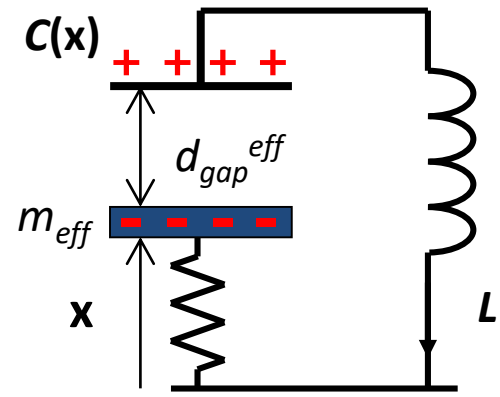
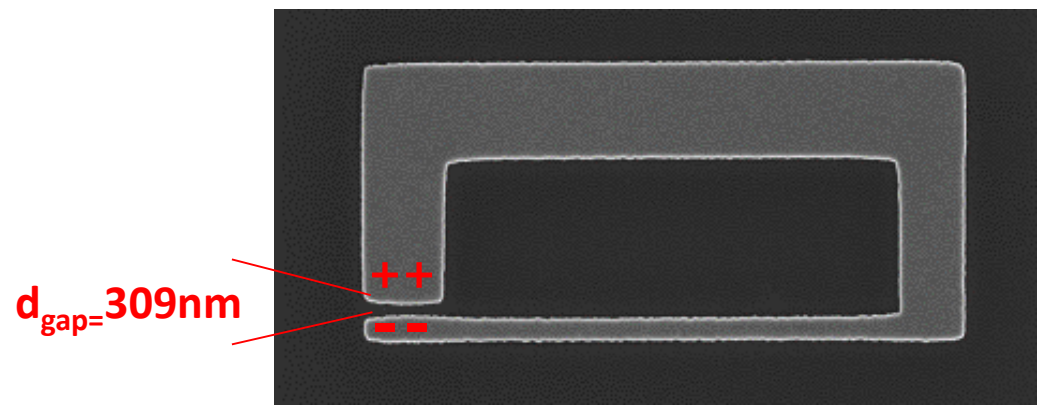
$$F_{\text{Coulomb}} = -W_{\text{THz}} \left. \frac{d \ln C_{\text{eff}}}{dx} \right|_{x=d_{\text{gap}}}$$

b. Photo-thermal (bolometric) interaction.



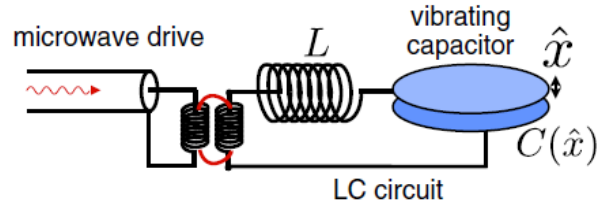
Electro-mechanical interaction: Coulomb force

non-bolometric force

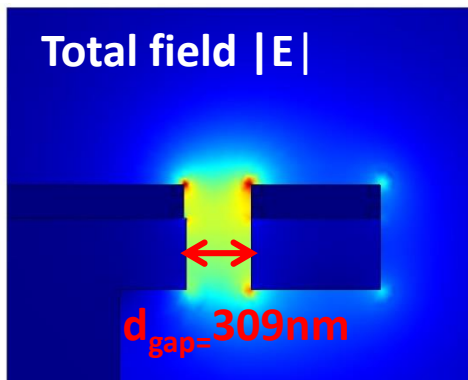
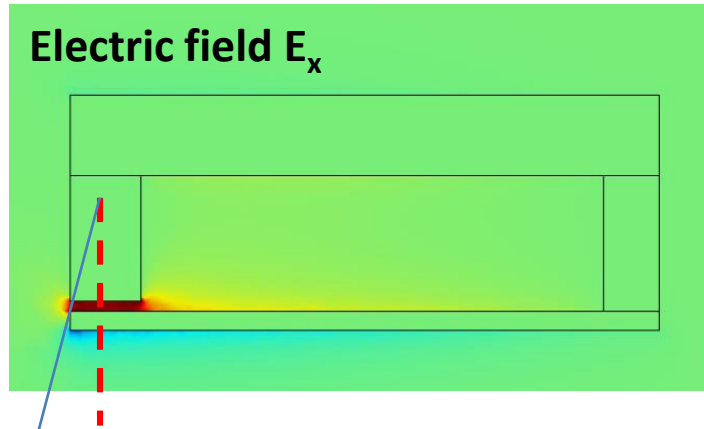


$$\frac{d^2 x}{dt^2} + \frac{\omega_m}{Q_m} \frac{dx}{dt} + \omega_m^2 x = - \frac{W_{THz}(t)}{m_{eff}} \left. \frac{d \ln C_{eff}}{dx} \right|_{x=d_{gap}}$$

Stored electric THz energy



Electro-mechanical interaction: Coulomb force: « non-bolometric »



$$d_{gap}^{eff} = \left(\left. \frac{d \ln C_{eff}}{dx} \right|_{x=d_{gap}} \right)^{-1}$$

$$d_{gap}^{eff} = 800\text{nm}$$

THz force for **1nW** of coupled power:

$$W_e = \frac{1}{2} P Q_{THz} / \omega_{THz} \sim 1.8 \times 10^{-22} \text{ J}$$

$$F_{Coulomb} = W_e / d_{gap}^{eff} = 0.2 \text{ fN}$$

$$\text{Stiffness: } k = m_{eff} \omega_m^2 = 0.4 \text{ N/m}$$

$$x = F_{Coulomb} / k = 0.5 \text{ fm} \dots$$

... But if the oscillator is resonantly driven with $Q_m = 100$:

$$x_{max} = Q_m F_{THz} / k = 50 \text{ fm}$$

Electro-mechanical interaction: Coulomb force: « non-bolometric »

Figures of merit

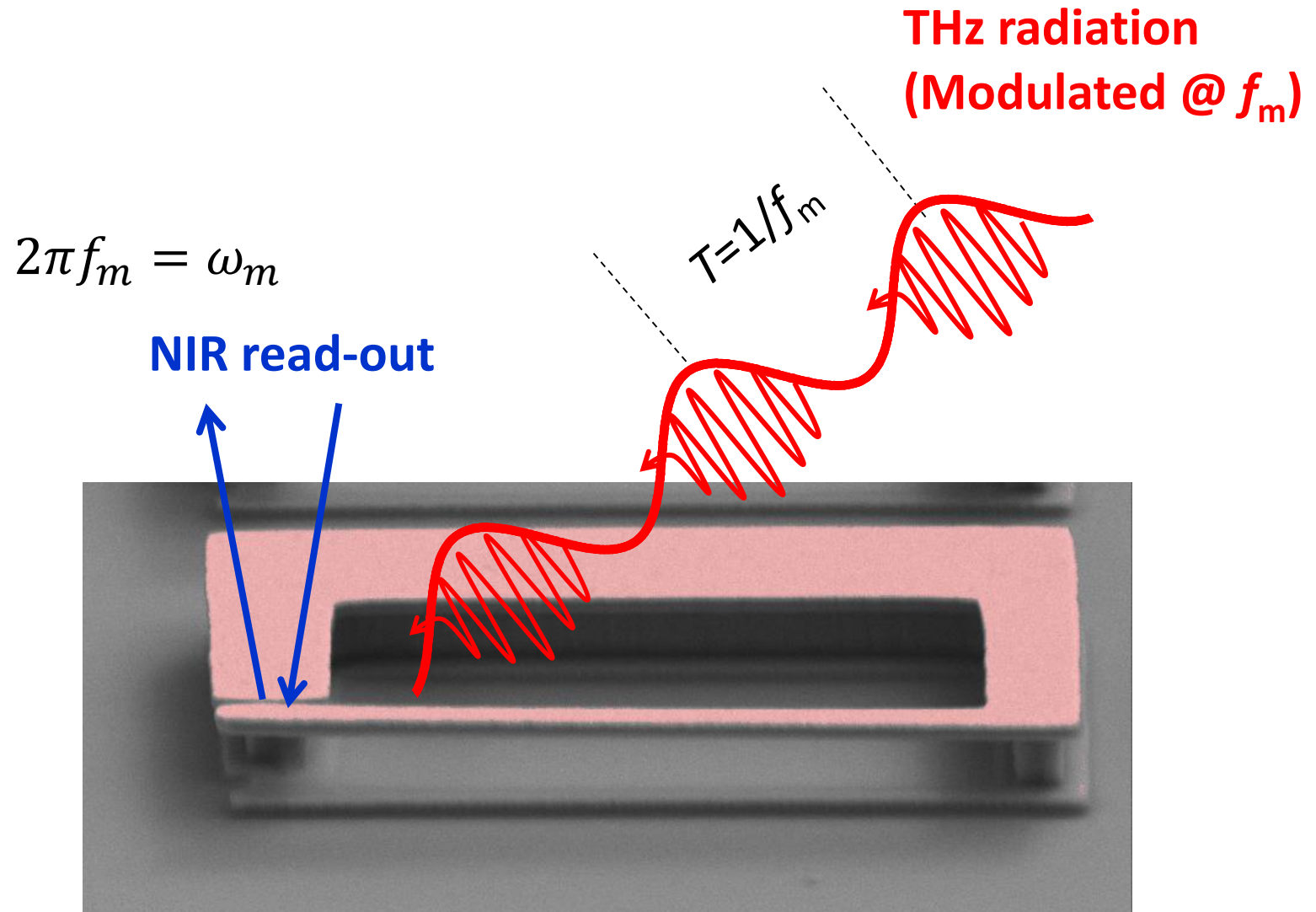
$$R_{in} = \frac{x_{\max}}{P_{THz}} = \frac{Q_m}{2m_{\text{eff}}\omega_m^2} \frac{Q_{THz}}{d_{\text{gap}}^{\text{eff}}\omega_{THz}} \sim \mathbf{50 \text{ fm/nW}}$$

$$NEP = \frac{\sqrt{S_{xx}(\omega_m)}}{R_{in}} = \sqrt{2k_B T m_{\text{eff}} \frac{\omega_m}{Q_m} \frac{2\omega_{THz} d_{\text{gap}}^{\text{eff}}}{Q_{THz}}} \sim \mathbf{10 \text{ nW/Hz}^{0.5}}$$

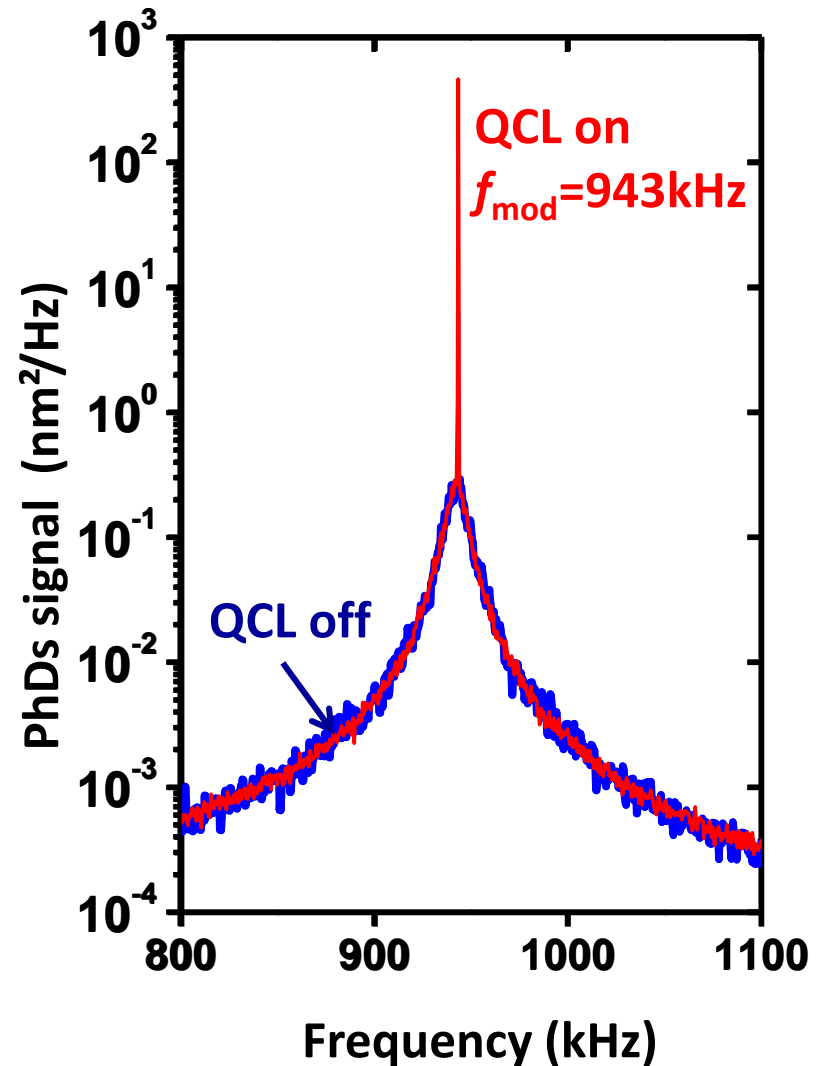
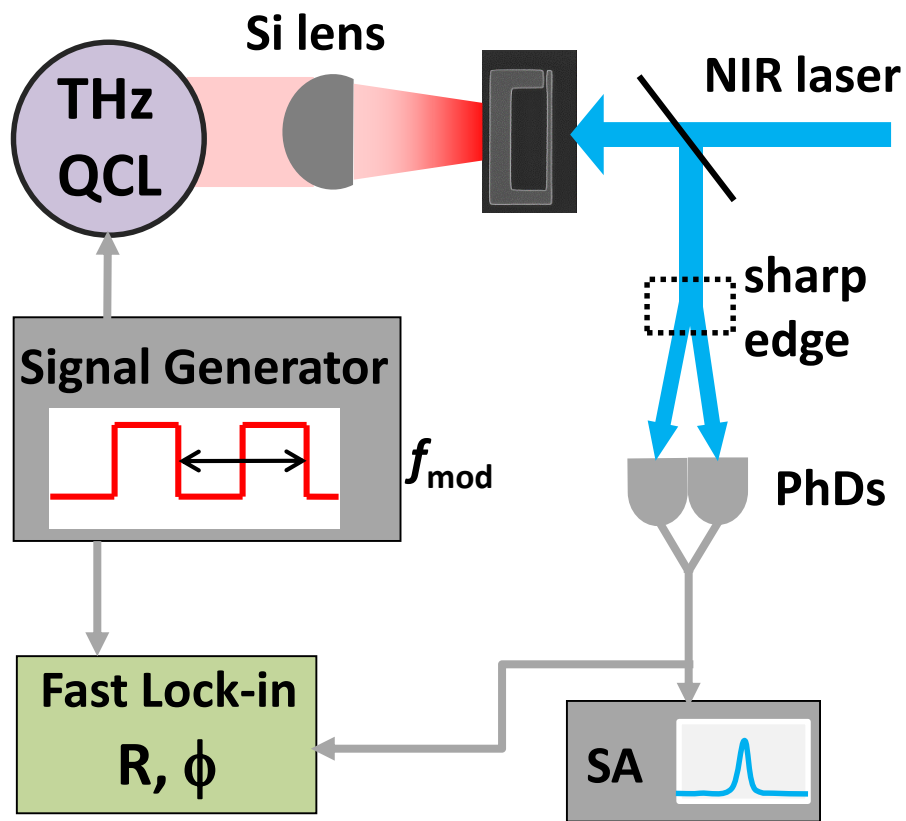
@ 1 MHz and higher

THz detection

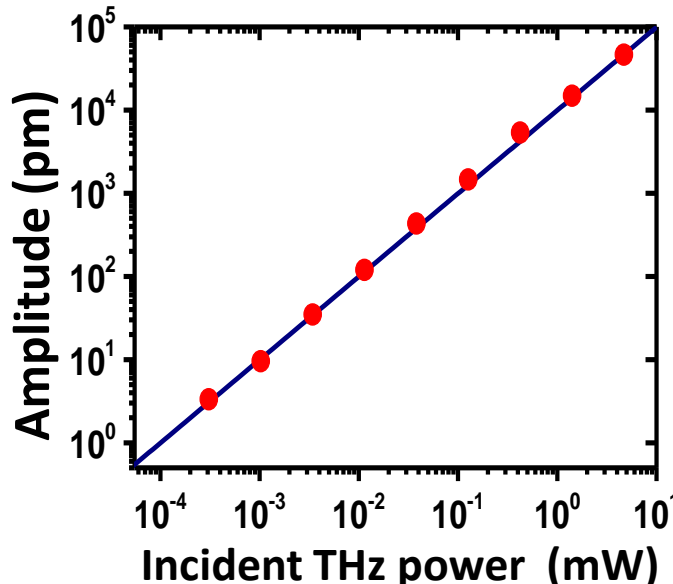
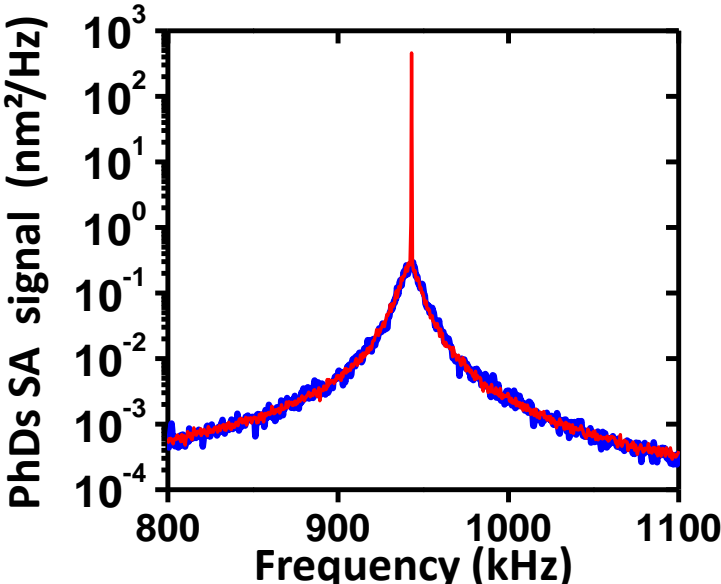
Principle of operation



THz optomechanical signal



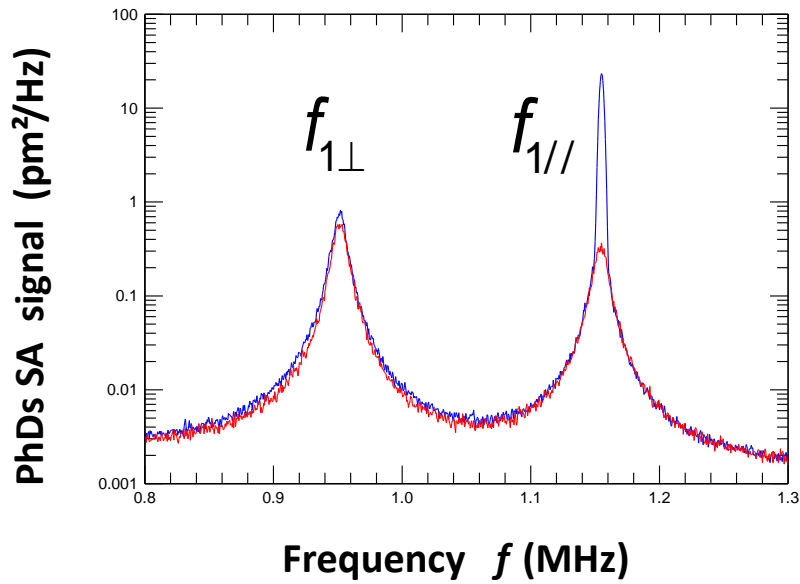
Performance as a detector



**Brownian motion
limited NEP: 8 nW/Hz^{1/2}**

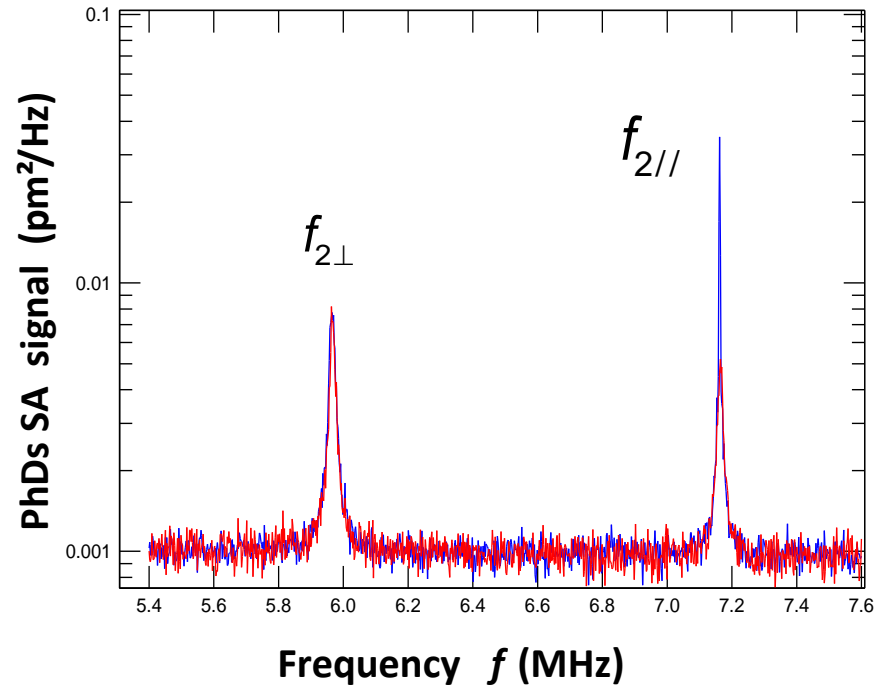
Performance as a detector

Electro-mechanical mechanism



$$R_{\text{exp}} \sim 5 \text{ fm/nW}$$

$$\text{NEP}_{\text{exp}} \sim 80 \text{ nW/Hz}^{0.5}$$



$$\text{NEP}_{\text{exp}} \sim 90 \text{ nW/Hz}^{0.5}$$

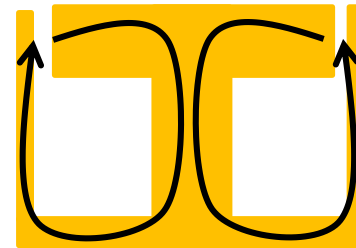
Going further?

$$NEP = \sqrt{2k_B T m_{eff} \frac{\omega_m}{Q_m} \frac{2\omega_{THz} d_{gap}^{eff}}{Q_{THz}}}$$

More
symetry to
decrease
radiation
loss

In air:
 $Q_m \sim 70$

In vacuum:
 $Q_m \sim 2000$



$Q_{THz} \sim 100$

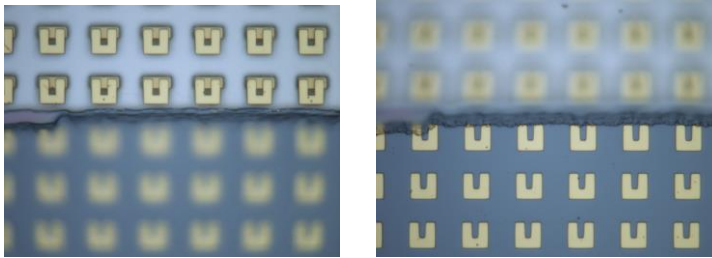
Al-Naib, et al.

Appl. Phys. Lett. **106**, 011102 (2015)

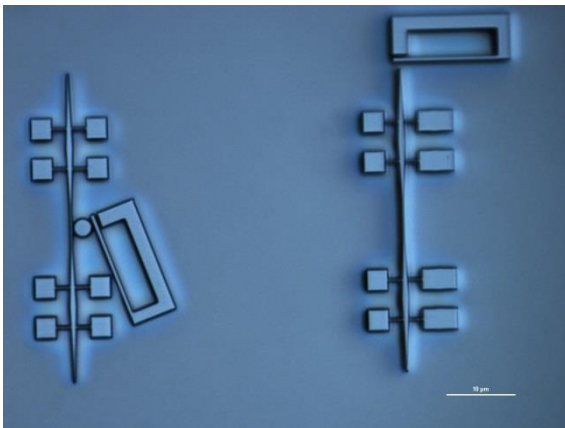
NEP <100pW/Hz^{0.5} is within reach

Conclusion & Perspectives

I. THz metamaterial resonators have strong potential for improving the temperature operation of quantum detectors



II. Towards compact THz optomechanical metamaterial sensors



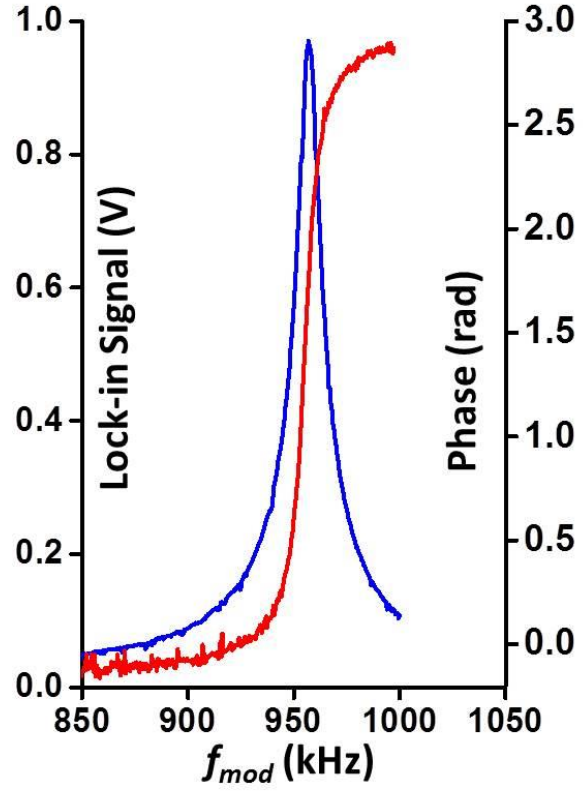
Opto-mechanical interaction within *single* sub-wavelength resonator

« Material free concept » OK for Si

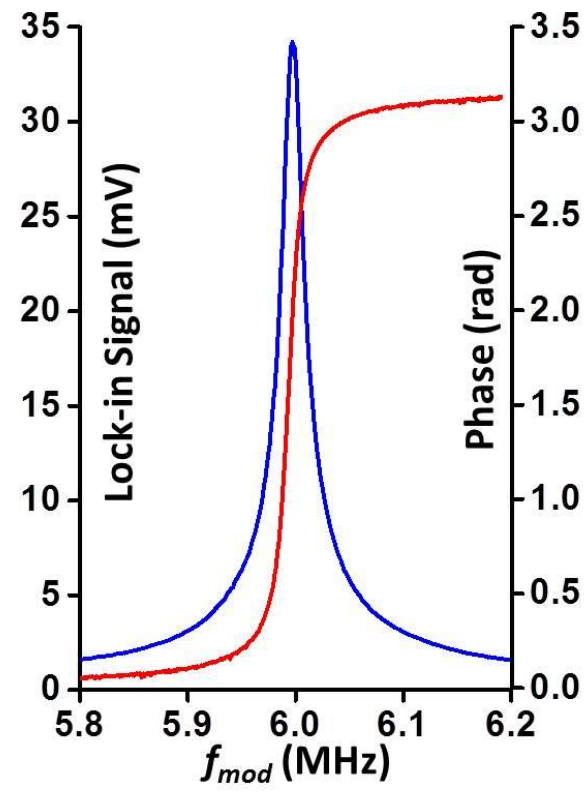
Scanning the modulation frequency



1st order



2nd order



3rd order

